CONTROL OF CELL DIVISION BY NUTRIENTS, AND ER STRESS SIGNALING IN *Saccharomyces cerevisiae*

A Dissertation

by

JINBAI GUO

Submitted to the Office of Graduate Studies of
Texas A&M University
in partial fulfilment of the requirements for the degree of

DOCTOR OF PHILOSOPHY

May 2007

Major Subject: Genetics

CONTROL OF CELL DIVISION BY NUTRIENTS, AND ER STRESS SIGNALING IN *Saccharomyces cerevisiae*

A Dissertation

by

JINBAI GUO

Submitted to the Office of Graduate Studies of
Texas A&M University
in partial fulfilment of the requirements for the degree of

DOCTOR OF PHILOSOPHY

Approved by:

Chair of Committee,	Michael Polymenis
Committee Members,	Donald W. Pettigrew
	Rodolfo Aramayo
	Mary Bryk
Chair of Intercollegiate Faculty,	James R. Wild

May 2007

Major Subject: Genetics

ABSTRACT

Control of Cell Division by Nutrients, and ER Stress Signaling in *Saccharomyces cerevisiae.* (May 2007)

Jinbai Guo, B.S., Northeast Agriculture University; M.S., Harbin Medical University

Chair of Advisory Committee: Dr. Michael Polymenis

Cell cycle progression of *Saccharomyces cerevisiae* cells was monitored in continuous cultures limited for glucose or nitrogen. The G1 cell cycle phase, before initiation of DNA replication, did not exclusively expand when growth rate decreased. Especially during nitrogen limitation, non-G1 phases expanded almost as much as G1. In addition, cell size remained constant as a function of growth rate. These results contrast with current views that growth requirements are met before initiation of DNA replication, and suggest that distinct nutrient limitations differentially impinge on cell cycle progression. Therefore, multiple mechanisms are hypothesized to regulate the coordination of cell growth and cell division.

Genetic interactions were identified between the dose-dependent cell-cycle regulator 2 (*DCR2*) phosphatase and genes involving in secretion/unfolded protein response pathway, including *IRE1*, through a genome-wide dominant negative genetic approach. Accumulation of unfolded proteins in the endoplasmic reticulum triggers the unfolded protein response (UPR). How the UPR is downregulated is not well understood. Inositol requirement 1 *(IRE1*) is an endoplasmic reticulum transmembrane

UPR sensor in *Saccharomyces cerevisiae*. When the UPR is triggered, Ire1p is autophosphorylated, on Ser 840 and Ser 841, inducing the cytosolic endonuclease activity of Ire1p, thereby initiating the splicing and translational de-repression of *HAC1* mRNA. Homologous to Atf/Creb1 (Hac1p) activates UPR transcription. We found that that Dcr2p phosphatase functionally and physically interacts with Ire1p. Overexpression of *DCR2*, but not of a catalytically inactive *DCR2* allele, significantly delays *HAC1* splicing and sensitizes cells to the UPR. Furthermore, Dcr2p physically interacts in vivo with Ire1p-S840E, S841E, which mimics phosphorylated Ire1p, and Dcr2p de-phosphorylates Ire1p *in vitro*. Our results are consistent with de-phosphorylation of Ire1p being a mechanism for antagonizing UPR signaling.

DEDICATION

To my wife and daughter, Jing Wu and Claire Yaxuan Guo. Without their constant support, I might have gone astray in the journey.

ACKNOWLEDGMENTS

I give sincere thanks with all my heart to all the professors and colleagues in the Department of Biochemistry & Biophysics of Texas A&M University. Dr. Michael Polymenis was a fabulous advisor and mentor. His encouragement and advice made it possible for me to continuously and relentlessly explore the challenging field of science. He taught me how to do experimental science and his enthusiasm in science always impressed me on my Ph.D journey. I appreciate Dr. Donald W. Pettigrew, Dr. Mary Bryk and Dr. Rodolfo Aramayo for their help and encouragement. Their mentoring and support encouraged me, along with all of their valuable advices.

I acknowledge the help and support of the members of the Polymenis laboratory, including Dr. Lydia M. Bogomolnaya, Dr. Ritu Pathak, Dr. Bong- Kwan Han, James M. Totten, and Heidi M. Blank. Without their help, my graduate school experience would not have been so enjoyable. I convey my special thanks to Dr Lydia Bogomolnaya and Dr. Ritu Pathak, great friends and co-workers who have always been there to support and help me with experiments. James M. Totten and Heidi M. Blank are great helpers and labmates. I thank the members of the LiWang lab, the Kladde lab, the Bryk lab and the Shippen lab who have generously let me use facilities in their lab. I acknowledge the help and technical expertise of Ms. Jane Miller. I thank Julia Williams, the GENE graduate advisor, and Chara J. Ragland, the genetics TA advisor, for their help, and to the genetics program for recruiting me.

I thank all my friends, especially Libin Wang and Hongjun Jin. Finally, I want to thank my parents, who have been the mainstay of my success, my sister for their love and confidence, and my wife Jing, whose love and support keep me going.

I believe that Aggieland was a destination for my training, not only as a scientist but also as a human being. The last five years were full of learning and enlightenment in many ways.

TABLE OF CONTENTS

CHAPTER Page

LIST OF FIGURES

LIST OF TABLES

CHAPTER I

INTRODUCTION

Our laboratory is mainly interested in studying how cell division is tightly coupled with cell growth in all proliferating cells, using the budding yeast *Saccharomyces cerevisiae* as our model system. Budding yeast is a genetically tractable eukaryotic organism, whose genome has been sequenced. In particular, yeast is a great model system for cell cycle studies for two reasons: First, the fundamental mechanisms of cell cycle regulation are evolutionarily conserved between yeast and mammalian organisms; Second, the appearance of buds is a unique morphological marker to tell if cells are committed to a new round of cell division.

THE CELL CYCLE

The cell cycle, or cell-division cycle (CDC), consists of a series of continuous events, in which the cellular components are duplicated and ultimately equally segregated into two healthy and viable daughter cells. Based on the characteristics of cellular biology and physiology, mainly the behavior of chromosomes, the cell cycle of animal cells can be divided into four distinct phases: G1 phase, S phase, G2 phase (collectively known as interphase) and M phase. M phase is featured with chromosome condensation and equal segregation and ended in cytokinesis, in which the cytoplasm

---

This dissertation follows the style and format of Cell.

(containing cellular organelles) physically divides. The interphase involves obtaining nutrients, duplication of genetic material and organelles, reorganization of the cytoskeleton, and formation of the mitotic spindle. In G1 phase, the cell grows in mass and prepares for the next cell cycle; in S phase, the chromosomes are duplicated; in G2 phase, the cell continues to grow in preparation for cell division.

Likewise, the cell cycle of the budding yeast, *Saccharomyces cerevisiae*, can also be divided into four comparable phases under the same parameters, G1, S, G2 and M phase. Cells in G1 are sensitive to external stimuli, such as availability of nutrients and the presence of anti-mitogenic stimuli. Under poor nutrient conditions, cells arrest in the G1 phase, and diploid cells may undergo sporulation. Exposure to anti-mitogenic stimuli, such as mating pheromones, high salt conditions or some chemicals, arrests cells in late G1 phase. If the external environment is acceptable, cells grow to meet their physiological requirements until initiation of the next round of cell division. Hence, G1 phase is generally seen as the limiting step for overall cell proliferation, and the observation that cell proliferation rates correlate with the duration of G1 phase has led to the important concept of START (or the Restriction Point). START is a point in late G1 when various aspects of the cell's physiology are measured and monitored. Passage through START ensures that growth requirements are met before the cell is committed to the next division (Pringle and Hartwell, 1981). The completion of START is normally concomitant with the transition from G1 to S phase, which is marked with several landmark events like initiation of DNA replication, duplication of the microtubule-organizing center called a spindle pole body (SPB) and appearance of a bud on the

surface. Subsequently, chromosomes are duplicated in S phase; after G2 phase, cells proceed to M phase.

Budding yeast undergoes closed mitosis where the nuclear membrane remains intact throughout M phase (Murray and Hunt, 1993). The bipolar spindle is assembled inside the nuclear membrane, and the nucleus then divides into two nuclei after chromosome segregation. Mitosis ends with cytokinesis, where an asymmetric division gives rise to a smaller daughter cell and a larger mother cell (Hartwell and Unger, 1977).

CELL GROWTH AND CELL DIVISION

The general cellular parameters, such as overall cell size and macromolecular composition, remain relatively constant for all proliferating cells during successive cell division cycles. This is true for all living organisms (from bacteria to humans). These general cellular physiological phenomena strongly indicate the tight coordination between overall cell growth and cell division. However, the molecular mechanisms of how cell growth is tightly coupled with cell division are mostly unclear and debatable. The following illustrates how we view this question. (For simplicity, the discussion will be only focusing on unicellular organisms like budding yeast.)

For clarification and convenience, cell growth refers to increases of biomass (e.g., size and/or weight), measured as doubling time of total biomass.The rate of increase of macromolecules (e.g., total RNA and protein) but exclusive of DNA determines whether cell growth is fast or slow, and it is dependent on the total metabolic activity of cell. Cell division refers to the doubling of DNA, which is coupled to mitosis

once DNA synthesis begins. Fast or slow transition among four sequential cell division phases is determined by the duration of each phase relative to the overall doubling time. Thus, comparisons of cell cycle transitions can only be properly done when there is no significant difference of the overall doubling time. Following these definitions of cell growth and cell division, we could simplify three scenarios of how cell growth is coupled with cell division (Neufeld and Edgar, 1998; Polymenis and Schmidt, 1999): growth and division are independent of each other; division controls growth; or growth controls division. These are not mutually exclusive, and they may somehow integrate together, depending on different internal and external environments. I outline each scenario below.

First, cell growth and cell division may work in parallel during cell proliferation, in other words, they could work independently in some cases. Indeed, rat Schwann cell growth can continue to increase cell volume up to nearly 5 fold when cell division is blocked (Conlon and Raff, 2003), arguing that cell division does not control cell growth; Early *Xenopus* embryos can undergo 12 successive cell divisions without significant changes of overall biomass, arguing that cell growth is not limiting for cell division in early embryogenesis. Interestingly, cell size of budding yeast under continuous culture conditions does not vary as a function of the growth rate but as function of nutrient composition (Chapter III) (Guo et al., 2004). Therefore, the biomass or cell size cannot be the exclusive parameter to evaluate for the coordination of cell growth and cell division, though it does provide a useful parameters in pursuing this question. Most studies assume that unlike many key cell cycle regulators that oscillate throughout the

cell cycle, metabolsm does not oscillate during the cell cycle. Yet metabolic programs also display nice controlled periodic cycles, such as O_2 consumption, CO_2 excretion, NADH and H_2S (Lloyd et al., 2003; Lloyd and Murray, 2006; Tu et al., 2005; Tu and McKnight, 2006). Microarray studies reveal that essential cellular and metabolic events occur in synchrony with the metabolic cycle (Tu et al., 2005). It will be worth studying further the connection between cell cycle oscillation and metabolic cycles. Some genes, such as those targeted by *C-myc*, are known to control both cell growth and division (Polymenis and Schmidt, 1999).

Second, cell division might regulate cell growth during cell proliferation. The three G1 cyclins of budding yeast contribute differently to the fitness of the population in nitrogen-limiting continuous cultures (Bryan et al., 2004). Furthermore, loss of G1 cyclins, or inactivation of the cyclin-dependent kinase Cdc28p, reduced the activity of glutamate synthetase (Glt1p), a key enzyme in nitrogen assimilation, suggesting that completion of START may be linked to nitrogen metabolism (Bryan et al., 2004). Given that about 13% of non-histones, 20% of histone, 15.75% of DNA and 14.95% of RNA mass is nitrogen, it won't be a surprise that to initiate cell division, the cell needs to up-regulate nitrogen metabolism. Additionally, it might be a self-supporting mechanism, because cells need to guarantee that their biosynthetic requirements will be met for chromosome duplication and cell cycle completion, since passage through START is basically a commitment and "no return" action.

Third, cell growth controls cell division during cell proliferation. This scenario is very well accepted for the coordination of cell growth with cell division. In most cases,

when cell growth is limited, such as under poor nutrient conditions, there is not only an extension of the overall doubling time, but also it is most strikingly visible in the length of G1 phase, before DNA replication. In other words, cell division seems to be mostly controlled at the G1 phase. Therefore, it is believed that the cell cycle profile (more strictly, the duration of G1 phase) would be identical for cells growing at the same rate, because the critical growth rate and nutrient requirements have to be reached in G1 (Pringle and Hartwell, 1981). However, we demonstrate that the G1 phase of budding yeast only predominantly expands as the growth rate declines in glucose-limiting continuous cultures, but not in nitrogen-limiting continuous cultures, where all cell cycle phases appear to proportionally expand (not only G1). These results indicate that cell growth is controlled in a nutrient-specific manner and cannot be exclusively monitored at START (Chapter III) (Guo et al., 2004). Therefore, cell cycle phases besides G1 should be included in studies of coordination of cell growth and cell division, especially since cell growth is a continuous process. Cell growth limitations might primarily become evident in G1 simply because during the previous phases of cell cycle there is a continuous accumulation of molecules necessary for the G1/S transition.

CURRENT MODELS FOR COORDINATION OF CELL GROWTH WITH CELL DIVISION

Current studies of the coordination of cell growth with cell division are mostly focusing on size and G1 phase. It is thought that cells have to grow to a critical cell size before they can initiate division during the normal cell cycle. Budding yeast undergoes

asymmetric division, where the daughters are usually born smaller than the mothers, thus daughter cells have to spend more time in G1 phase to grow more to reach the critical size. This is thought to maintain size homeostasis. Protein synthesis and, in particular, ribosome biogenesis is thought to determine initiation of cell division, but the two prevailing models for such a control reach opposite conclusions.

The first model is called the "Cln3p abundance model". This model centers around the G1 cyclin Cln3p. Over-expressing *CLN3* induces a smaller size, shorter G1 phase, and START is accelerated. Conversely, deletion of *CLN3* leads to larger size, longer G1 and START is delayed. Note however that small or large cell size due to gain or loss of *CLN3* primarily derives from disproportional changes of vacuole size (Han et al., 2003), adding more complexity. Nonetheless, a short upstream open reading frame (uORF) in the 5' leader of *CLN3* mRNA causes its translational repression in media with a poor carbon source, when the concentration of ribosomes is low (Polymenis and Schmidt, 1997), thus delaying completion of START. Therefore, Cln3p can serve as an ideal mediator between growth conditions and the cell cycle machinery. However, as discussed previously, the length of G1 can be varied independent of growth rate and cell size (Chapter III), other phases need to be considered as well. Hence, modulation of Cln3p levels cannot fully explain the coordination of cell growth with cell division.

The second model is called the "nutrient modulation of critical cell size threshold model" (Jorgensen et al., 2004). The model proposed that increased ribosome content suppresses completion of START so that cells can grow to a larger size before they can initiate division; in contrast, ribosomal biogenesis mutants, with a decreased ribosome

content, can undergo cell division at a smaller size, thus passage through START is accelerated. However, *sfp1Δ* (encoding a transcription factor involved in expression of ribosomal proteins) and *sch9Δ* (encoding a kinase important for ribosome biogenesis) cells proliferate slowly, and their G1 phases are greatly prolonged: *sch9* mutants by 35% and *sfp1* mutants by 280% (Jorgensen et al., 2004). Thus, despite their small cell size, the timing of START is actually significantly delayed in these mutants compared to wild type.

The common questionable part of these two models is that they seemed only to stress one parameter but overlook another. The "Cln3p abundance model" uses the duration of G1 to evaluate fast or slow cell cycle progression, but ignores the cell size changes. On the other hand, the "nutrient modulation of critical cell size threshold model" only emphasizes the critical size, but overall proliferation is actually much slower than wild type.

From our previous discussion, it can be seen how complex this question is, and it can hardly be explained by one model. It won't be surprising if coordination of cell growth with cell division is regulated by multiple mechanisms, which might add "plasticity". One mechanism could be quickly switched to another, following internal or/and external changes of conditions, allowing for either cell growth or cell division to completely stop, while the other process is still ongoing. Unlike the well-controlled conditions in our research labs, cells, especially from unicellular organisms, need the ability to cope with unexpected "noise" in the environment. Interestingly, cells within a genetically-uniform population can exhibit striking phenotypic variability. Also, no

matter how well a cell population can be synchronized, they will be asynchronous again within a few rounds of divisions. Nevertheless, the tight coordination between cell growth and division determines when cells initiate cell division. Therefore, gene products, which can promote the completion of START, will definitely help us understand how the coordination is achieved.

SCREEN FOR NOVEL REGULATORS OF START

Previously, two types of genetic screens were done to identify regulators of START, which relied on cell size changes (Jorgensen et al., 2002; Prendergast et al., 1990; Sudbery et al., 1980; Zhang et al., 2002) and resistance to pheromone (Cross, 1988; Edwards et al., 1997; Reed, 1980). However, cell size can be regulated independently of cell cycle progression, and cells continue to grow in the presence of pheromone though they don't divide, thereby disturbing the normal coordination of cell growth with cell division. Thus, there must be other unknown factors involved the regulation of START.

Hence, a screen was performed in our lab to identify genes that shorten the G1 phase in a dosage-dependent manner. The screen used a novel mechanical enrichment procedure without significantly perturbing normal cellular physiology. It totally relies on the timing of START without depending on alterations of cell size or pheromone resistance (Bogomolnaya et al., 2004a). After the screen, several gene products were identified and shown to accelerate the G1/S transition when over-expressed. They are *GID8* (Glucose Induced Degradation), *DCR2* (Dosage dependent Cell cycle Regulator),

HYM1 (HYpha-like Metulae 1) and *KEM1* (Kar1-1 nuclear-fusion-defect Enhancing Mutation) (Bogomolnaya et al., 2004b; Bogomolnaya et al., 2006; Pathak et al., 2004; Pathak et al., 2005).

Dcr2p PHOSPHATASE

The Dosage-dependent Cell cycle Regulator gene *DCR2* contains a GNHD/E sequence motif, which is in the calcineurin-like metal-containing phosphoesterases (*E* value = $1e^{-5}$) (Geer et al., 2002), and thought to be important for the hydrolysis of phosphate esters in the active-site dinuclear metal center. Thus Dcr2p is a putative phosphatase. A histidine to alanine substitution in the GNHD/E motif still allows substrate binding but impairs catalytic activity in λ Ser/Thr phosphatase and calcineurin (Mertz et al., 1997) (Zhuo et al., 1994). When histidine 338 is mutated to alanine in Dcr2p's GNHD/E motif, a dominant-negative variant (Dcr2p-H338A, or $Dcr2p^{DN}$) is generated. Indeed, $Dcr2p^{DN}$ can significantly antagonize the wild type function of Dcr2p in accelerating cell cycle progression (Pathak et al., 2004). Further functional analysis indicated that *DCR2* and *GID8* work in a common pathway, in a dosage-dependent manner, to promote START (Pathak et al., 2004).

To further investigate the biological function of Dcr2p, a genome-wide genetic screen utilizing this dominant negative allele ($DCR2^{DN}$) was done. The screen intended to identify genes that have synthetic sick or lethal effects with *DCR2*, suggesting that genetically these two genes contribute towards the same biological function. Through this genome-wide dominant-negative approach, we interrogated 4,021 deletion strains.

Finally, 12 genes were validated to have genetic interaction with *DCR2*. Nine of them have putative roles in trafficking and unfolded protein response caused by ER stress, indicating a physiological function of Dcr2p.

ER STRESS

The endoplasmic reticulum (ER) plays an essential role in the biosynthesis of proteins destined for secretion or membrane insertion in eukaryotes (Back et al., 2005; Schneider et al., 2004). This membrane-bound organelle, which associates with translating ribosomes and translocates peptides into its lumen, is a processing plant to promote a variety of post-translational modifications and chaperone-facilitated folding events. Proteins must be correctly folded and assembled in the ER prior to transit to intracellular organelles and the cell surface. In addition, by serving as the primary site at which client proteins enter the secretory compartment and as the site of synthesis and assembly of the lipid bi-layer, the ER indirectly controls the capacity and scope of the entire endomembrane/endocytic system. Therefore, the endoplasmic reticulum is exquisitely sensitive to alterations of cellular homeostasis. At any given time, the load of client proteins that the ER must handle is kept at a balance with trafficking of client proteins into the secretory pathway that the ER should promote, which is set by developmental programs and modulated by physiological stimuli. As a result, when the influx of nascent, unfolded polypeptides exceeds the folding and/or processing capacity of the ER, and/or if the secretory processes are blocked, the normal physiological state of the ER is perturbed, resulting in the accumulation of unfolded proteins in the ER. This

is called ER stress, primarily due to the toxic effect of the accumulating unfolded proteins, which constitutes a fundamental threat to the cells. In other words, ER stress is defined functionally as an imbalance between the load of client proteins facing the ER and the organelle's ability to process that load.

ER stress can be triggered under a number of cellular stress conditions, such as perturbations in calcium homeostasis or redox status, sugar/glucose deprivation, elevated protein synthesis, expression of misfolded proteins and blocked secretory pathway (Lee, 1992). Mutations impairing the client protein folding or chemicals that disturb the protein folding can cause ER stress (Gething and Sambrook, 1992), such as blocking glycosylation with tunicamycin, or inhibiting disulfide bond formation with dithiothreitol. Since ER is the site of the synthesis of sterols and lipids, the perturbations in lipid metabolism can also cause an ER stress response, but very little is known about the mechanism of its activation by perturbations in lipid metabolism. In mammals, ER stress can be provoked by a variety of pathophysiological conditions, for example, ischemia, hyperhomocystinemia and viral infections (Aridor and Balch, 1999; Kaufman, 1999). The phenotypes resulting from mutations affecting components of the ER stress response machinery reveal that ER stress is also a normal physiological phenomenon (Harding et al., 2001).

UNFOLDED PROTEIN RESPONSE

Eukaryotic cells have evolved specific signaling pathways and effector mechanisms to deal with ER stress. By the late 1980s, it had been known that there is a

specific link between manipulations that perturb protein folding in the ER and the induction of a class of mRNAs that encode ER chaperones (Hendershot et al., 1988; Kozutsumi et al., 1989; Kozutsumi et al., 1988). Although this gene expression program was highly reminiscent of the well characterized heat-shock response, which couples perturbation in the folded state of cytoplasmic proteins with the activation of genes that restore homeostasis to the cytoplasmic folding environment, the ER chaperone–encoding genes are not induced by heat shock (Kozutsumi et al., 1988). This suggests the presence of a compartment-specific signaling pathway that couples events in the lumen of the ER to changes in gene expression in the nucleus. Because this trans-organelle signaling pathway is activated experimentally by manipulations that impede protein folding in the ER or by expression of mutant ER client proteins impaired in their ability to fold, it was named the unfolded protein response (UPR) signaling pathway. Now it is believed that the UPR signaling pathway is more likely triggered by the threat of their accumulation, not by the malfolded/unfolded proteins themselves.

Because of the nature of ER stress, the UPR signaling pathway should primarily serve for one major mission, that is to re-balance the load of client proteins with the capacity of ER, thus recovering ER homeostasis. Therefore, UPR signaling should be able to (1) sense the signals of ER stress; (2) transduce them into effectors; (3) turn on target genes. It can also be imagined that there are likely two ways for the UPR signaling pathway to recover the normal status of ER, either by promoting protein folding inside the ER and boosting secretion from the ER, or by decreasing the loading of protein into

the ER, such as attenuating protein synthesis. Indeed, all the UPR signaling pathways identified so far, have exactly these characteristics.

Several components of the UPR have been identified during the last decade. They either integrate in a linear pathway or work in a parallel manner. The basic components of the UPR pathway were first characterized in the budding yeast, *Saccharomyces cerevisiae,* in the early 1990s. Ire1p/Ern1p, which was first identified in a genetic screen for Inositol Requiring genes in budding yeast, is an ER transmembrane protein kinase/endoribonuclease. It is a transducer that initiates UPR signaling and it is essential for cell survival during ER stress (Cox et al., 1993; Mori et al., 1993). Thereafter, researchers found that all eukaryotic cells have conserved the essential and unique properties of Ire1p-mediated UPR signaling pathway as the one identified in yeast, but also evolved additional transducers to generate a diversity of responses. In mammals, the counterpart of yeast Ire1p has two isoforms: IRE1α and IRE1β. Whereas IRE1α is expressed in most cells and tissues, IRE1β expression is primarily restricted to the intestinal epithelial cells (Hemminki et al., 1998; Welihinda et al., 1998). In addition to IRE1, higher eukaryotic cells have two additional UPR transducers: the double-stranded RNA-activated protein kinase-like ER kinase (PERK) and activating transcription factor 6 (ATF6). The UPR signaling pathways include both translational and transcriptional responses. Overall, translational response is mediated by PERK; transcriptional response is mediated through ATF6 and IRE1.

PERK contains a large ER luminal stress-sensing domain that is functionally interchangeable with the IRE1 luminal domain and a cytosolic kinase domain. When ER

stress is sensed from the ER lumen, PERK can specifically phosphorylate the αsubunit of eukaryotic translation initiation factor 2 (eIF2α) on Serine 51 (Harding et al., 1999; Liu et al., 2000). This phosphorylation of eIF2α inhibits eIF2B, the GTP exchange factor, to change GDP-binding form of eIF2α into GTP-binding form (Dever, 2002), thus repressing the reutilization of eIF2α and initiation of translation. Therefore, one direct consequence of the phosphorylation of eIF2α by PERK upon ER stress is to attenuate translation activities globally, thus decreasing the protein load to the ER. This is a very convenient and efficient way to control translation initiation, coupling stress response signaling pathways to block cellular protein synthesis through eIF2α (Harding et al., 2002). For example, the typical analogue is that GCN2 and HRI phosphorylate eIF2α in amino acid starved cells. Interestingly, some UPR target genes, such as ATF4, have several small open reading frames at their 5′ end, called upstream open reading frames (uORFs), which mediate basal repression of their translation. Under conditions of eIF2α phosphorylation, these mRNAs are translated more efficiently (Scheuner et al., 2001). Thus, another consequence of phosphorylation of eIF2α by PERK upon ER stress is to specifically up-regulate a certain group of UPR target genes.

ATF6, a member of the ATF/CREB protein family, is a transcription factor with an N-terminal basic leucine zipper (b-ZIP) domain in the cytosol and a C-terminal ER luminal domain to sense stress (Haze et al., 1999). ATF6 is constitutively synthesized as an ER membrane protein. The ER membrane-associated ATF6 is inactive for transcription. When the signals of ER stress are sensed from the ER lumen, ATF6 is first translocated into the Golgi apparatus. Then, its cytosolic domain, containing the DNA-

binding and transcriptional activation domains, is proteolytically cleaved off and then transported to the nucleus to specifically activate transcription of UPR target genes (Yoshida et al., 2000).

IRE1-MEDIATED UPR SIGNALING PATHWAY

The *IRE1*-mediated UPR signaling pathway, first identified in *Saccharomyces cerevisiae*, is evolutionarily conserved in eukaryotic organisms (from yeast to mammals), and plays a central role in ER stress. In both budding yeast and mammals the pathway works in an almost identical manner. It is mainly composed of an ER transmembrane protein kinase (Ire1p) and a specific bZIP transcription factor, Hac1p in yeast or XBP-1 in humans, serving as a downstream target (Zhang and Kaufman, 2004).

Ire1p localizes across the ER membrane and can be dissected into three functional domains. First, the amino-terminal domain resides in the ER lumen, and plays a major role in sensing the accumulation of unfolded proteins. Second, after the transmembrane linker region of Ire1p, there is an atypical serine/threonine kinase domain in its upper cytosolic region, which phosphorylates itself in trans after being activated. Third, the C-terminal tail is an endoribonuclease domain showing strong homology to RNase L.

The mechanism of how Ire1p's ER-lumenal domain (LD) senses unfolded proteins is still controversial. Both yeast Ire1p LD's and human IRE1α LD's crystal structures have been solved recently (Credle et al., 2005; Zhou et al., 2006), and they are very similar. This is not a surprising since there is high degree of conservation between

their amino acid sequences. Both of them adopt the formation of the MHC-like groove. However, the size of the groove of human Ire1p LD is too narrow to permit peptide binding as being proposed from yeast Ire1p LD, and the key residues in the groove also function differently. Nevertheless, both crystal structures support the notion that homo-dimerization or oligomerization (possibly through direct interaction with unfolded proteins) is the prerequisite step for activating the response, because mutations on their surfaces of dimerization compromise the response. Interestingly, there is a constitutively ON version of *IRE1* in yeast, called $IRE1^{C}$, which carries mutations in its LD region (Travers et al., 2000). Therefore, both biochemical and genetic analysis indicate that UPR activation has to be initiated from Ire1p's LD; additionally, a common mechanism of activation is likely to exist due to the fact of functionally exchangeable ER lumenal domain among yeast Ire1p, human Ire1p and even human PERK (Liu et al., 2000).

After the signal of accumulating unfolded proteins is sensed and UPR activation is initiated by the Ire1p ER lumenal domain, Ire1p's dimerization (or oligomerization) is triggered across the ER membrane (See the figure on page 24). This results in optimal and close positioning of Ire1p Ser/Thr kinase domains in the cytoplasm. These domains are then autophosphorylated in *trans*, which is supported both by intragenic complementation analysis between some *IRE1* alleles and direct physical interactions among the cytosolic regions (Shamu and Walter, 1996; Welihinda and Kaufman, 1996). For example, in budding yeast, an *ire1* allele missing the C-terminal tail, still maintains kinase activity but not endonuclease activity, and it is able to complement the UPR activity of an *ire1* kinase-dead allele, still having intact C-terminal tail and endonuclease

activity. Such intragenic complementation also provides strong evidence for dimerization or oligomeriztion of Ire1p during the UPR. The autophosphorylation primarily happens on S840 and S841. Although *in vitro* data also show that T844 is phosphorylated, its physiological significance is unclear. In contrast, the dual phosphorylations at S840 and S841 are absolutely required for normal function of the UPR signaling pathway *in vivo*. In budding yeast, when both of Serines are substituted into Alanines, making non-phosphorylatable variants, UPR signaling is essentially eliminated. The mutant is very sick under ER stress and phenotypically behaves like an *ire1* null (Guo and Polymenis, 2006; Shamu and Walter, 1996). Therefore, phosphorylation is critical for the physiological function of the *IRE1*-mediated UPR; it also potentially provides a way to down-regulate UPR activity *in vivo*.

Dual phosphorylation at S840 and S841 is believed to lead to a conformational change of Ire1p's cytosolic domain, which further activates the C-terminal tail's endoribonuclease activity towards its sole substrate, the *HAC1* mRNA (Niwa et al., 2005; Sidrauski and Walter, 1997) (See the figure on page 24). The conformational change of *IRE1* cytosolic domain and activation of its C-terminal tail nuclease activity can also be achieved through association of small molecules. For instance: *in vitro*, adenosine 5'-diphosphate (ADP) or nonhydrolyzable ATP analog (AMP-PNP) can activate Ire1p* (the recombinant cytosolic portion of Ire1p), but not guanosine 5'-triphosphate (GTP) (Sidrauski and Walter, 1997); more interestingly, *in vivo*, the ATP-competitive drug 1-tertbutyl-3-naphthalen-1-ylmethyl-1H-yrazolo[3,4-d]pyrimidin-4-ylemine (1NM-PP1) can restore UPR activity of the Ire1 kinase-dead variant—Ire1p (L745G) (which only

has ~10% UPR activity). The replacement of Leu745—located at a conserved position in the adenosine 5'-triphosphate (ATP)–binding site—to Ala or Gly is predicted to sensitize Ire1p to the 1NM-PP1 by creating an enlarged active-site pocket (Bishop et al., 1998; Papa et al., 2003). Regardless of how it can be activated, all the data indicate that the C-terminal tail nuclease activity is directly under the control of the Ire1p cytosolic kinase domain. Finally, given the low or zero UPR activity of non-phosphorylatable and kinase dead variants of Ire1p, the phosphorylation event must be required for the normal function of *IRE1*-mediated UPR signaling pathway *in vivo*.

Overall, upon ER stress, the three functional domains of Ire1p are activated sequentially across the ER membrane after initiation inside the ER lumen. In other words, *IRE1* itself is both a primary sensor and a transducer, playing dual roles in the UPR signaling pathway (See the figure on page 24). Consequently, modulating *IRE1* activity would have a direct impact on the UPR, generating the most effective way to manipulate the UPR.

HAC1 UNCONVENTIONAL SPLICING AND TRANSLATIONAL CONTROL

Hac1p was first identified as a basic leucine Zipper (bZIP) transcription factor homologous to Atf/Creb1 (Nojima et al., 1994). At about the same time, *HAC1* was found in two screens for high copy suppressors of the inositol auxotrophic phenotype of the *ire1* mutation that restore UPR activity of *ire1* mutants, which also indicate that *HAC1* may function downstream of *IRE1* (Cox and Walter, 1996; Nikawa et al., 1996). Interestingly, Hac1p protein was only detected in UPR-on cells, while its mRNAs were

present in both UPR-on and UPR-off cells at comparable levels (Cox and Walter, 1996; Kawahara et al., 1997). These *HAC1* mRNAs are respectively named as *HAC1*^{u} ("u" for *u*ninduced , UPR-off state) and *HAC1*^{i} ("i" for *i*nduced, UPR-on state) mRNA. Consequently, the proteins encoded by these two forms of *HAC1* mRNA are called Hac1p^{u} and Hac1p^{i}, respectively. The *HAC1*^{i} mRNA is formed by the removal of a 252 base pair intron from the *HAC1*^{u} mRNA by a non-conventional splicing mechanism, because the splicing process is spliceosome-independent but Ire1p-dependent. Activated ER transmembrane kinase/endonuclease Ire1p can specifically cleave both 5'- and 3'-exon-intron junctions in *HAC1*^{u} mRNA (Sidrauski and Walter, 1997). The 5'- and 3'-portions of the mRNA are re-joined by the tRNA ligase, Rlg1p. An *rlg1* temperature sensitive mutant is totally defective in UPR and splicing of *HAC1* mRNA (Sidrauski et al., 1996) (See the figure on page 24).

Three lines of evidence indicate that the expression of Hac1p is essentially controlled at the translation level. First, *HAC1*^{u} mRNA is primarily detected in the cytoplasm (Chapman and Walter, 1997), thus ruling out that *HAC1*^{u} mRNA is retained in the nucleus. Second, a large portion of *HAC1*^{u} mRNA co-migrates with polyribosomes in sucrose gradients and can be immunoprecipitated with an antibody against an N-terminal epitope, demonstrating that the N terminus of the protein is made and exposed outside the ribosome (Chapman and Walter, 1997; Cox and Walter, 1996); These results also suggest that translation of Hac1p^{u} is initiated, but those ribosomes then stall on the mRNA before translation is completed. Third, the Hac1p^{u} produced by intronless constructs has a similar half-life of Hac1p^{i} in yeast cells ($t_{1/2}$ ~2 min)

(Chapman and Walter, 1997; Kawahara et al., 1997), suggesting that fast protein degradation is unlikely. Because *HAC1*^{u} mRNA is barely translated but *HAC1*^{i} mRNA is translated promptly and efficiently after splicing, the spliced intron may play a key role in limiting translation of *HAC1*^{u} mRNA. Indeed, further studies demonstrate that the intron region of *HAC1*^{u} mRNA not only forms stem-loop-like secondary structure itself but also bends towards its 5′-UTR region with base-pairing interactions (See the figure on page 24). Thus, the intron and the 5'-UTR need to work together for blocking translation of *HAC1*^{u} mRNA (Ruegsegger et al., 2001). These unique RNA structures prevent ribosomes from reading through after initiation of translation, stalling *HAC1*^{u} mRNA in polyribosome state. Therefore, the only way to release the translational block of *HAC1*^{u} mRNA is to remove its intron specifically by activated Ire1p. Also, because of how translation is blocked, the Hac1p protein is literally already "half made". Thus, Hac1p^{i} is produced rapidly upon the activation of Ire1p, which explains quite well why UPR can be turned on in a very short time, only taking about 10 minute after experimental induction in yeast (See the figure on page 24).

Mutated X-box binding protein-1 (XBP-1), the mammalian counterpart of *HAC1*, was first shown to block the UPR in *C. elegans*. Activation of the UPR causes *IRE1*-dependent splicing of a small intron from the XBP-1 mRNA both in *C. elegans* and mice. The protein encoded by the processed murine XBP-1 mRNA accumulated during the UPR, whereas the protein encoded by unprocessed mRNA did not (Calfon et al., 2002; Shen et al., 2001). So far, *HAC1* or XBP-1, are the only substrates of yeast Ire1p or human Ire1p nuclease, respectively (Calfon et al., 2002; Cox and Walter, 1996; Niwa

et al., 2005). Both splicing events are induced by the activation of Ire1p in responding to the accumulation of unfolded proteins in the ER lumen (Bertolotti et al., 2000; Cox et al., 1993; Shamu and Walter, 1996).

HAC1-MEDIATED UPR TARGET GENES

Hac1p^{u} and Hac1p^{i} are identical except for their C-terminal tails. Splicing replaces a tail of 10 amino acids encoded in the intron of *HAC1*^{u} mRNA with a tail of 18 amino acids encoded in the second exon of *HAC1*^{i} mRNA. Therefore, removal of the *HAC1* intron not only allows translation of the mRNA but also alters the sequence and properties of the encoded protein. The DNA-binding domain in the N-terminal 220 amino acids common to Hac1p^{i} and Hac1p^{u} is undisturbed during the splicing, but the C-terminal *trans*-activation domain is altered. The C-terminal tail of Hac1p^{i} served as a very highly active transcriptional activation domain, while the Hac1p^{u} tail was essentially inactive, after fusing them to an unrelated DNA-binding domain (Kawahara et al., 1997; Mori et al., 2000). Thus, splicing also results in a stronger transcription factor, Hac1p^{i} (Figure 1.1).

Hac1p^{i} is responsible for activating transcription of a large set of UPR target genes in yeast (~5% of the genome). The majority of them encode gene products involved in protein folding, such as *KAR2* and *PDI*; ER-associated protein degradation (ERAD) components, such as *DER1*and *HRD3*; and many proteins that function downstream in the secretory pathway (Travers et al., 2000). This large set of up-regulated genes fits well with the goal of the UPR signaling pathway to cope with ER

stress. Although Hac1p^{i} expression is sufficient for induction of several ER target genes, Hac1p^{i} also needs to recruit some or all of the components of the SAGA complex, a multiprotein assembly involved in histone acetylation during transcriptional activation, to the promoters of UPR target genes; this interaction is necessary for full induction of a subset of targets (Welihinda et al., 1997). Interestingly, one component of the SAGA complex, Ada5p, appears to interact with the cytosolic domain of Ire1p and be required *in vivo* for the splicing of *HAC1* mRNA (Welihinda et al., 2000). Additionally, *HAC1* mRNA transcription is also regulated through an Ire1p-independent pathway, adding more levels of complexity in UPR signaling (Patil et al., 2004).

So far, three *cis*-acting promoter elements regulated by Hac1p have been identified. They are: (1) the unfolded protein response element (UPRE, CAGNGTG) (Mori et al., 1992). It is the major regulatory element of Hac1p, found in the promoters of ER chaperone genes; most of UPR target genes have UPRE on their promoters, but some ER-associated protein degradation genes are regulated by Hac1p in a UPRE-independent manner. Mammalian UPR target genes also carry consensus promoter sequence, called ER stress-response element (ERSE, CCAATN$_9$CCACG), which are regulated by XBP-1 and ATF6 (Yoshida et al., 1998). (2) subtelomeric ATF/CREB GTA variant element (SACE, ATGGTATCAT) (Spode et al., 2002); (3) the upstream repressing sequence 1 (URS1, TCGGCGGCT), found in the promoters of early meiotic genes and many genes involved in carbon and nitrogen utilization; it makes Hac1p^{i} the first bZIP transcription factor in yeast that both activates and represses transcription (Schroder et al., 2004).

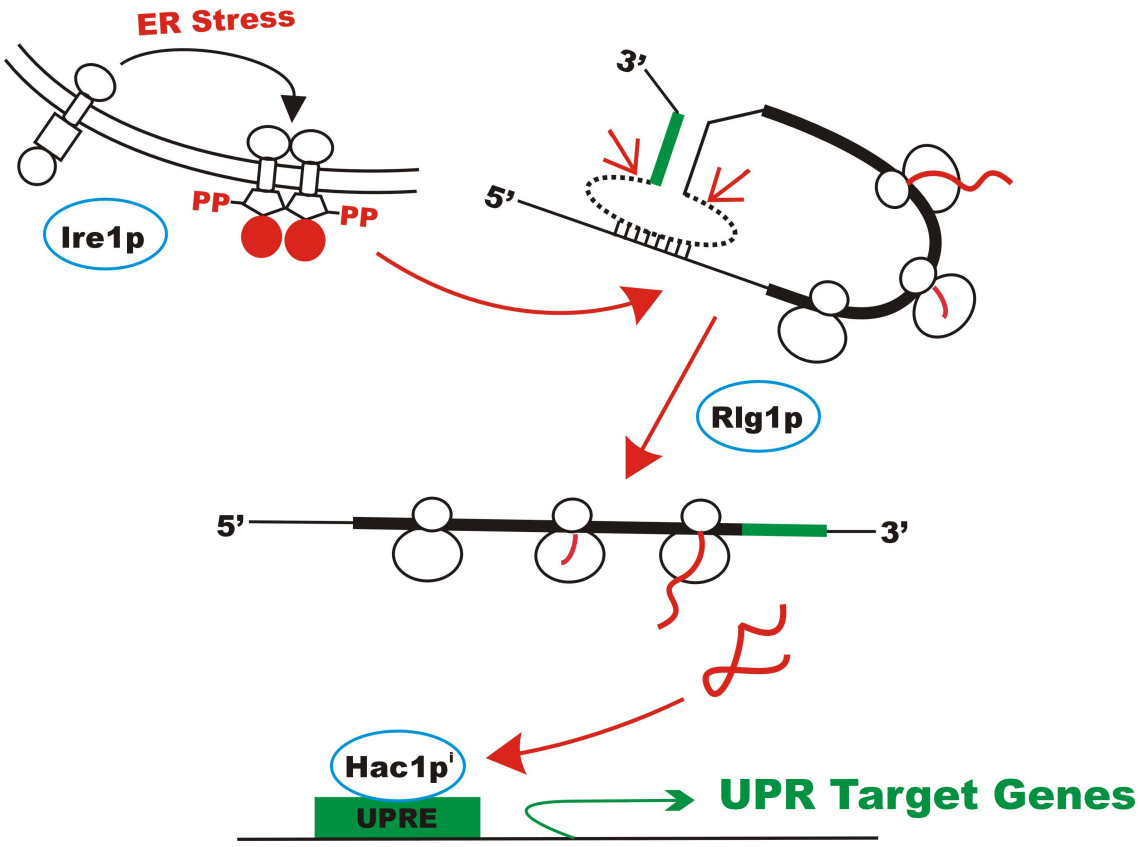

Figure 1.1 The unfolded protein response signaling pathway in *Saccharomyces cerevisiae*

UPR IS ANTI-MITOGENIC

It has been known since the 1980s that tunicamycin, an inhibitor of protein N-glycosylation that also induces the UPR, would eventually cause cell-cycle arrest in both yeast and human lymphoma cells. This occurred in the G1 to S transition and blocked DNA synthesis (Arnold and Tanner, 1982; Nishikawa et al., 1980; Savage and Baur, 1983). In yeast, constitutive expression of the intron-less *HAC1*^{i} transcript significantly delays cell proliferation (Kawahara et al., 1997). It might be partially explained by the association of Hac1p^{i} with the URS1 primary transcriptional repressor Ume6p, a Zn_2Cys_6 cluster protein. Ume6p can cause the repression of ~10% to ~20% of all yeast genes; the majority of them are involved in metabolism, such as carbon and nitrogen utilization (Strich et al., 1994).

In mammalian cells, there is clear evidence that experimental induction of the UPR in mouse NIH 3T3 fibroblasts with tunicamycin leads to a decline in cyclin D- and E-dependent kinase activities and to G1 phase arrest (Brewer et al., 1999). The loss of cyclin D1 appears to be directly mediated by the kinase activity of PERK upon activation of UPR (Brewer and Diehl, 2000). Furthermore, sustained activation of the UPR could eventually trigger programmed cell death (Apoptosis), and all three known UPR signaling pathways may be directly involved (Wu and Kaufman, 2006). For example, activated Ire1p binds to the c-Jun-N-terminal inhibitory kinase (JIK) and recruits TRAF2 (TNF receptor-associated factor-2), which leads to the activation of ASK1 (apoptosis signal-regulating kinase 1)/JNK (c-Jun amino terminal kinase), and also to the release of the procaspase-12 from the ER, activating the caspase cascade

(Nakagawa et al., 2000; Nishitoh et al., 2002). CHOP (CEBP homologous protein), one of the UPR downstream effectors activated by both PERK/eIF2α/ATF4 and AFT6, inhibits the expression of Bcl-2 and thus promotes mitochondria-dependent apoptosis (Ma et al., 2002).

Overall, the UPR is anti-mitogenic and pro-apoptotic. Due to the ultimate deleterious effects to growing cells, mechanisms that down-regulate the UPR must exist. However, compared to what is known about how the UPR can be activated and turned on, very little is known about how it can be down-regulated and turned off. There is only *in vitro* evidence that the Ptc2p phosphatase might be an Ire1p phosphatase in budding yeast (Welihinda et al., 1998), but there is no functional *in vivo* interactions between Ire1p and a phosphatase.

Interestingly, in our genetic screen to further explore the physiological function of the Dcr2p phosphatase, among 12 genes obtained from the screen, 9 genes have putative roles in protein trafficking. These 9 genes are *RIC1, YPT6, SWA2, VPS54, TFP1, VPS51, SFH1, IRE1, PTC1* (Chapter IV). Protein trafficking defects trigger the UPR (Patil and Walter, 2001). Both *RIC1* and *YPT6* were already known to have genetic interactions with *DCR2*. Ric1p acts as a GTP exchange factor for the Ypt6p GTPase, regulating intracellular trafficking (Siniossoglou et al., 2000). *SWA2* and *VPS54* are likely UPR target genes because of their fairly good expression pattern correlation value to the known UPR target genes, 0.944 and 0.965 respectively (Travers et al., 2000). Finally, we demonstrated that *ire1* is synthetically lethal with *dcr2*; the Dcr2p phosphatase de-phosphorylates Ire1p *in vitro*, and interacts physically with Ire1p *in vivo*,

and down-regulates the unfolded protein response in *Saccharomyces cerevisiae* (Chapter IV).

UPR MODULATION IS NECESSARY

The UPR signaling pathway is an elaborate mechanism to ensure that only properly folded and assembled proteins exit the ER, a process termed "quality control." Increasing evidence indicates that the UPR needs to be activated even in cells considered healthy or unstressed due to variable internal environments. For example, the UPR signaling pathway is required in cells with defective ER-associated degradation (ERAD) in yeast and mammalian cells (Hori et al., 2004; Lee et al., 2003; Travers et al., 2000). UPR signaling in unstressed cells also appears to play a role in nutrition sensing and differentiation programs. The major molecular chaperones of the ER, BiP/GRP78 and GRP94, are induced by glucose starvation or anaerobiosis in mammalian cell (Pouyssegur et al., 1977), suggesting that the UPR is responsive to the nutritional state. Abrogation of PERK signaling through introduction of a *Ser51Ala* mutation into eIF2α in mice resulted in hypoglycemia associated with defective gluconeogenesis and a loss of the pancreatic β-cell population. The mice died within 18 hr after birth, which indicates that intact UPR signaling is critical for *in vivo* glucose homeostasis (Scheuner et al., 2001). During terminal differentiation of B cells into antibody-secreting plasma cells, XBP-1 is required and splicing of XBP-1 mRNA was observed (Calfon et al., 2002; Iwakoshi et al., 2003; Reimold et al., 2001).

Furthermore, in yeast, the level of UPR activation in unstressed cells is tightly linked to the metabolic state of the cell. A low level of *HAC1* splicing is observed in exponentially growing yeast in nitrogen-rich media (Schroder et al., 2000). Depending on carbon sources, between 3% and 30% of *HAC1* mRNA were detected in term to total *HAC1* mRNA. It is low on preferred, fermentable carbon sources (D-glucose and D-fructose), intermediate on disaccharides (D-maltose), and high on nonfermentable carbon sources, (acetate or ethanol). In addition, upon nitrogen starvation, the UPR can be turned off quickly in less than 5min. On the other hand, upon ER stress induced by tunicanmycin, splicing of *HAC1* can be sustained for more than 3 hours after the stress is removed (Chapter IV). It suggests that the UPR signaling pathway must be modulated in a subtle manner. It is possible that, depending on what signal is sensed, the UPR could be either activated in an unstable UPR-on/off status, likely involving in nutrient sensing or differentiation, or a stable UPR-on status, likely dealing with ER stress and even triggering apoptosis. Overall, UPR modulation is also necessary for "unstressed" cells, in addition to the stressed conditions.

However, how UPR can be modulated is still mysterious, since very little is known about how to turn it off. We obtained clear evidence, both *in vitro* and *in vivo*, that Dcr2p attenuated the UPR by directly targeting Ire1p in budding yeast (Chapter IV). Given that both gain- and loss-of-function *DCR2* alleles sensitized cells to tunicamycin; over-expression of *DCR2* could significantly delay *HAC1* splicing, but not block it; and Dcr2p is modified under ER stress in a time-dependent fashion, Dcr2p might work as a UPR modulator, possibly required for both off- and continuous on-state of UPR.

The pathogenic roles of the UPR are steadily drawing more and more attention. Viral infections activate the UPR (Tardif et al., 2005), and rapidly growing cancer cells rely on the UPR for their survival (Reimold et al., 1996). To understand more about how the UPR can be turned off would extend our knowledge about all these important cellular events, and potentially lead to the development of antiviral or chemotherapeutic cancer agents.

CHAPTER II

MATERIALS AND METHODS

Cell cultivation, media preparation and yeast molecular biology techniques were performed as described by Kaiser et al (Kaiser et al., 1994), unless otherwise indicated.

STRAINS AND DNAs

The *Saccharomyces cerevisiae* standard strains were obtained from the Yeast Genetic Stock Center, Calif., USA, others were generated from these standard strain genetic backgrounds in our lab for particular purposes. Most of the strains used in this study are listed in Table 2.1.

The *IRE1-S840A/S841A* and *IRE1-S840E/S841E* strains were generated by transformation of the wild type strains (BY4741 and BY4742) with the PCR-products bearing the two amino acid mutations and marked by the *HIS3* gene (Kaiser et al., 1994). The PCR-products were generated by amplification of plasmid P_{GAL1}-*IRE1-TAG* with the following oligonucleotide primers respectively:

S840A/S841A Forward 5'-

AATTTTGATATCAGACTTTGGTCTTTGCAAAAAACTAGACTCTGGTCAGGCT

GCATTTAGAACAAATTTGAATAACCCTTC–3',

S840E/S841E Forward 5'-

AATTTTGATATCAGACTTTGGTCTTTGCAAAAAACTAGACTCTGGTCAGGAG

GAATTTAGAACAAATTTGAATAACCCTTC-3'.

Ire1(+3516) Reverse 5'-GTCTGTCGGGTAGTTTATGTAGGGATG-3'

Table 2.1 *Saccharomyces cerevisiae* strains and their relevant genotypes

Strain	Relevant genotype	Source
BY4741	*MAT*a *his3Δ leu2Δ met15Δ ura3Δ*	Res. Genetics
BY4742	*MAT*α *his3Δ leu2Δ met15Δ ura3Δ*	Res. Genetics
BY4743	BY4741/BY4742	Res. Genetics
W303a	*MAT*a *ade2 trp1 leu2 his3 ura3 can1*	B. Futcher
X2180-5B	*MATa SUC2 mal mel gal2 CUP1*	ATCC
ire1Δ	*ire1* Δ::*kanMX* (BY4742 otherwise)	Res Genetics
SCMSP59	*PGAL-SIK1*::*HIS3* (BY4741 otherwise)	(Bogomolnaya et al., 2004a)
ABXL-1D	*MAT*a, *FLO1*, *gal1*	Res. Genetics
SCMSP49	Ura^- derivative of ABXL-1D	(Bogomolnaya et al., 2004a)
SCMSP87	P_{GAL}-*HYM1*::*his3MX/HYM1*$^+$ (BY4743 otherwise)	(Bogomolnaya et al., 2004b)
LBY1	*Hym1Δ*::*his3MX* (W303 otherwise)	(Bogomolnaya et al., 2004b)
SCMSP67	*cln3Δ*::*URA3 hym1Δ*::*his3MX* (W303 otherwise)	(Bogomolnaya et al., 2004b)
SCMSP63	P_{GAL}-*ACE2*::*his3MX* (W303 otherwise)	(Bogomolnaya et al., 2004b)
SCMSP114	P_{GAL}-*ACE2*::*his3MX cln3Δ*::*URA3 hym1Δ*::*LEU2* (W303 otherwise)	(Bogomolnaya et al., 2004b)
SCMSP86	P_{GAL}-*ACE2*::*his3MX cln3Δ*::*URA3* (W303 otherwise)	(Bogomolnaya et al., 2004b)
SCMSP73	P_{GAL}-*ACE2*::*his3MX hym1Δ*::*LEU2* (W303 otherwise)	(Bogomolnaya et al., 2004b)
LBY1(P_{GAL}-*CLN3*)	*hym1Δ*::*his3MX* [P_{GAL}-*CLN3*-CEN *URA3*] (W303 otherwise)	(Bogomolnaya et al., 2004b)
W303(P_{GAL}-*CLN3*)	[P_{GAL}-*CLN3*-CEN *URA3*] (W303 otherwise)	(Bogomolnaya et al., 2004b)

Table 2.1 (Continued)

Strain	Relevant genotype	Source
SCMSP74	*P $_{GAL}$–KEM1*::*his3MX* (BY4741 otherwise)	(Pathak et al., 2005)
SCMSP81	*P $_{GAL}$–KEM1::his3MX/KEM1* $^{+}$ (BY4743 otherwise)	(Pathak et al., 2005)
4540	*kem1*Δ::*kanMX* (BY4741 otherwise)	Res. Genetics
SCMSP75	P_{GAL}-*GID8*::*his3MX/GID8*$^{+}$ (BY4743 otherwise)	(Pathak et al., 2004)
SCMSP76	P_{GAL}-*DCR2*::*his3MX/DCR2*$^{+}$ (BY4743 otherwise)	(Pathak et al., 2004)
RPY3	P_{GAL}-*DCR2*::*his3MX* (BY4741 otherwise)	(Pathak et al., 2004)
SCMSP112	*gid8Δ*::*URA3 dcr2Δ*::*his3MX* (BY4741 otherwise)	(Pathak et al., 2004)
6576	*gid8* Δ::*kanMX* (BY4741 otherwise)	Res. Genetics
RPY1	*dcr2* Δ::*his3MX* (BY4741 otherwise)	(Pathak et al., 2004)
SCMSP116	*gid8* Δ::*URA3* (BY4741 otherwise)	(Pathak et al., 2004)
SCMSP131	*cln3* Δ::*kanMX gid8* Δ::*URA3 dcr2* Δ::*his3MX* (BY4741 otherwise)	(Pathak et al., 2004)
SCMSP123	*cln3* Δ::*kanMX gid8* Δ::*URA3* (BY4741 otherwise)	(Pathak et al., 2004)
10366	*cln3* Δ::*kanMX* (BY4742 otherwise)	Res Genetics
ptc1Δ	*ptc1* Δ::*kanMX* (BY4742 otherwise)	Res Genetics
ire1S840A/S841A	*IRE1-S840A/S840A* His (BY4741 otherwise)	(Guo and Polymenis, 2006)
ire1S840E/S841E	*IRE1-S840E/S841E* His (BY4741 otherwise)	(Guo and Polymenis, 2006)

The plasmid was list in Table 2.2. The *pET-28a(+)-Ire1** was a gift from Peter Walter (Papa et al., 2003). *Ire1** is cytosolic portion of *Ire1* with fully functional kinase and endonuclease domain. The plasmid P_{GAL1}-$DCR2^{DN}$ was generated through co-transformation and recombination in wild type strain (BY4743) with linearized plasmid 2μ $DCR2^{DN}$ cut by restriction endonuclease and PCR-product of amplification from genomic DNA of *pGAL1-DCR2* strain by the following oligonucleotide primers:

DCR2-(+1213)-Forward: 5'-CGGTTGGTAAAATTTATCCTGG-3'

DCR2-(+2223)-Reverse: 5'-CTGATGTCGCAGGACGAGTC-3'

The plasmid was finally sequenced to verify the introduced mutation and the absence of any other mutations at the Genome Technologies Laboratory of Texas A&M University.

Table 2.2 Plasmids and their relevant characteristics

Plasmid	**Relevant characteristic**	**Source**
DCR2	2μ [*DCR2*] *URA3*	(Pathak et al., 2004)
$DCR2^{DN}$	2μ [$DCR2^{DN}$] *URA3*	(Pathak et al., 2004)
pBAD-DCR2	[P_{BAD}-*DCR2-TAG*] *URA3*	This study
pBAD-$DCR2^{DN}$	[P_{BAD}- $DCR2^{DN}$-*TAG*] *URA3*	This study
BG1805-DCR2	2μ [P_{GAL1}-*DCR2-TAG*] *URA3*	Open Biosystems
BG1805-IRE1	2μ [P_{GAL1}- *IRE1-TAG*] *URA3*	Open Biosystems
pGAL1-$DCR2^{DN}$	2μ [P_{GAL1}-$DCR2^{DN}$] *URA3*	This study
*PET-28a(+)-Ire1**	[P_{T7}-*Ire1*-6XHis*] Amp	P Walter

MICROSCOPY AND FLOW CYTOMETRY

For microscopic examination of nuclear morphology, the cells from each indicated growth rates of either nitrogen or glucose limitation chemostats were stained with DAPI, 4',6-diamidino-2-phenylindole, from Molecular Probes (Ore.). The protocols we followed are from the Botstein laboratory, as described at http://genome-www.stanford.edu/group/botlab/protocols.htm. The stained cells were examined under a UV filter for nuclear morphology. Lastly, the evaluation of cell cycle progression is based on bud size and nuclear morphology as described previously (Bogomolnaya et al., 2004a).

DNA contents were obtained by flow cytometry as described previously (Haase and Lew, 1997), except that cells were stained with Sytox green (1 mM; Molecular Probes, Ore., USA) instead of propidium iodide. This resulted in higher quality DNA content profiles, in which the G1 and G2/M histogram peaks were sharp and well separated (see the figure on page 50), allowing for more accurate quantitative measurements. To generate the DNA content histograms, the same number of cells (30,000) was collected for any given growth rate and nutrient limitation, and the percentage of cells in G1 (indicative of the length of the G1 phase) was calculated from the DNA histograms using the ModFit software (Verity Software House, Me., USA). Although estimates of S phase duration (rigorously defined as the interval between the earliest and latest events of DNA synthesis from origins of DNA replication) were obtained, they are not reported because it is thought that flow cytometry may under-represent the actual duration of S phase (Haase and Lew, 1997). Note also that it was not

possible to distinguish G2 from M phase cells based on flow cytometry data. These considerations, however, did not impact on the objective of this study, because the duration of non-G1 phases (S, G2, M) were collectively compared to that of G1.

Briefly, the procedure for flow cytometry analysis of DNA content is the following: cells ($1x10^7$ cells/ml) were fixed overnight in an Ethanol-PBS solution (mixed at a 7:3 ratio); they were then re-suspended in 50 mM sodium citrate buffer (pH 7.0). The sample was treated with RNaseA (0.25 mg/ml) overnight at 37 °C. Finally, the sample was re-suspended in a 50 mM sodium citrate buffer (pH 7.0) containing 1 mM Sytox Green and sonicated for 10 seconds, immeadiately before it was evaluated by flow cytometry.

CHEMOSTAT AND NUTRIENT LIMITATION MEDIA

Chemostat conditions were similar to those reported previously (Baganz et al. 1997). A VirTis (Gardiner, N.Y., USA) chemostat with a 600-ml working volume was used. Temperature (30°C), airflow (2 l/min), stirring speed (300 rpm) and pH (5.5) remained constant in all experiments. The filtered minimal media contained 1.7 g yeast nitrogen base (without amino acids and ammonium sulfate)/l (Difco, Mich., USA). Glucose-limited media had 0.8 g dextrose/l (Quality Biosources, Tx., USA) and 5 g ammonium sulfate/l (Fisher Scientific). Nitrogen-limited media had 20 g dextrose/l and 0.5 g ammonium sulfate/l. No sample was taken from the chemostat for further analysis unless the cells were cultured for at least five generations at any given dilution rate.

Viability of samples taken from the chemostats was evaluated on solid rich media, containing 10 g yeast extract/l, 20 g peptone/l and 20 g dextrose/l.

Cell cycle progression was evaluated in chemostats in which the growth, or dilution (D), rate can be altered separately from nutrient-dependent variables simply by altering the speed of the pump that introduces fresh medium in the culture. The reasons are the following: A chemostat is a completely mixed continuous stirred-tank reactor (CSTR), in which the medium is pumped continuously and the volume is constant since the excess medium overflows, so the conditions in the reactor do not change with time. Therefore, when equilibrium is established inside the reactor, the rate of production of cells equals to the rate of loss of cells though overflow (K*X=D*X, so K=D, K is growth rate, D is dilution rate). In other words, a chemostat can be used to run the reactor at particular growth rate by controlling the feed rate into the reactor. (Book, "Physiology of the Bacterial Cell: A Molecular Approach" by Frederick C. Neidhardt, John L. Ingraham, Moselio Schaechter; Sinauer Associates Inc, June 1990).

CELL SIZE MEASUREMENT

Cell size was measured using a Beckman Coulter Z2 Channelyzer. Each time the Channelyzer needs to be flushed three times before use. The samples were sonicated to disperse clumps prior to analysis, which was further confirmed by microscopic examination. The data were analyzed using the manufacturer's AccuComp software. The reported values are based on the geometric mean of the cell size distribution of each

sample. Besides the cell size, the Channelyzer also gives the cell density at the same time.

BUDDING INDEX AND DOUBLING TIME MEASUREMENTS

The percentage of budded cells (budding index) was evaluated as described elsewhere (Zettel et al., 2003). Because of the unique feature of budding yeast that the appearance of a bud is concomitant with completion of START, the percentage of unbudded cells corresponds to the relative duration of G1 phase and the percentage of budded cells equals to non-G1 phase when the overall doubling time is the same. The budding index is the fraction of budded cells in a population. In this sense, for equal overall doubling times, a high budding index is indicative of a shorter G1 phase, so cell cycle progression is accelerated; low budding index is indicative of a longer G1 phase, so cell cycle progression is delayed. Budding index usually expressed as relative values, compared to its control strain (usually wild type strain) at any given time.

Briefly, one needs to grow at least 20 inoculations of one strain into exponential phase, reaching at least 10^6 cells/ml, then count budded cells microscopically with a hemacytometer, in order to calculate the budding index and do statistics.

There are two ways to measure the population doubling (generation) time in these studies. One is to use the absorbance at 595nm (A) obtained with a spectrophotometer at multiple time points (t) during the exponential growth of the culture, which is particularly useful for strains with a segregation defect strain, such as *hym1Δ*. The other one is to use the Beckman Coulter® counter Channelyzer to measure

the cell density at multiple time points (t) during the exponential growth of the culture. These values can be plotted against time (t), to obtain both the slope (k) and linear regression value (R^2) of the line. When R^2 is between 1 and 0.9, the k is taken. The culture's doubling time (g) is then calculated from the formula $g = \ln 2/k$. For each particular strain, doubling times were measured at least three times.

These two experiments, budding index and doubling time, were done for all the strains studied in these papers (Bogomolnaya et al., 2004a; Bogomolnaya et al., 2004b; Bogomolnaya et al., 2006; Pathak et al., 2004; Pathak et al., 2005).

IMMUNOFLUORESCENCE MICROSCOPY

For the subcellular localization of Gid8p and Dcr2p in the paper (Pathak et al., 2004), we used cells expressing alone epitope-tagged Gid8p-HA, Dcr2p-Myc, or co-expressing Gid8p-HA and Dcr2p-Myc, and two untagged controls (BY4742 for the HA-tagged strains or BY4741 for the Myc-tagged strains, BY4743 for the co-expressing strain). Cells were grown into mid-log phase in 5 ml YPD. We then add 0.5 ml 37% formaldehyde and incubated at 30°C for 1h. The cells were centrifuged and resuspended in Sorbitol Buffer (0.5ml 40mM KPO_4 (pH6.5), 500µM $MgCl_2$, 1.2M Sorbitol). We then added 100 µl of a 3 mg/ml Zymolyase (20T) solution, and incubated for 30~45 min at 30°C. The cells were then washed once with Sorbitol Buffer, then resuspended in 100~500 µl Sorbitol Buffer. A 25µl cell suspension were then spotted on a polylysine-coated slide and incubated at room temperature for 10 min. The slide was plunged into a container with ice-cold methanol for 6 min, then plunged into another container with ice-

cold acetone for 30 sec. The slide was then immediately placed against a slanted, flat, warm, clean surface so that the acetone could evaporate without the creation of condensation. The slides were then blocked in PBS pH 7.4 with 1% BSA Tween 20 for 15min at room temperature. The cells were incubated in primary antibody at the appropriate dilution in block solution for 1h at RT; washed 4 times for 5min per time; incubated in secondary antibody conjugate (either FITC or TRITC) diluted in block solution for 1h at RT. The slides were washed again and mount solution was added (100mg p-phenylenediamine in 10ml PBS, add volume to 100 mls with glycerol pH=8.0) with 50ng/ml DAPI.

Immunofluorescence microscopy followed the protocols of the Botstein lab as described at http://genome-www.stanford.edu/group/botlab/. The samples were examined with a Nikon Eclipse TS100 inverted fluorescence microscope.

BACTERIAL EXPRESSION

The *pBAD-DCR2-TAG*, and *pET-28(a)-IRE1**, plasmids were transformed into *E. coli* XL1-Blue, and BL21, respectively. For protein expression we followed previously published procedures (Guzman et al., 1995; Nock et al., 2001). Briefly, five or six colonies were used to start a 50 ml preculture in Luria-Bertani (LB) medium, containing either 50µg/ml Ampicillin (for *pBAD-DCR2-TAG*) or 100µg/ml Kanamycin (for *pET-28(a)-IRE1**). The precultures were grown for 14h to late log phase and used to inoculate larger batches at a dilution of 1:200 in LB medium. The larger batch volume we used was 1L, shaking flasks (225 rpm) at 37°C to an OD_{600} of 0.6 to 0.8. For the

pBAD cultures, we induced with 1% Arabinose sitting on the bench overnight at RT. For the *pET-28(a)-IRE1** cultures, we induced with 0.7mM isopropyl-β-D-thiogalactopyranoside (IPTG) at 30°C for 4h. After induction, the cultures were placed in the cold room (4°C) overnight. Lastly, cells were harvested by centrifugation with a GSA rotor at 16,000g at 4°C for 15min, and stored in -80°C for cell lysis by french press.

FRENCH PRESS LYSIS

The 1L cell pellet were resuspended in 15ml Buffer A (20 mM HEPES pH7.5, 150 mM KCl, 1 mM dithiothreitol (DTT), 5mM $MgCl_2$, 10% (v/v) glycerol) containing complete Mini©, EDTA-free protease inhibitor cocktail tablets (Roche Diagnostics) (Nock et al., 2001). All the components of the french press (outlet valve, lid, plunger and cell) were cooled down. A spot of glycerol was applied onto the rubber seals, then the plunger and lid were placed into the cell, and the outlet valve was fitted. It was then left open and the cells were loaded into the press cell. The cell was placed into the press, the clamp across the cell was closed to lock it in place and the two screws were tightened by finger. The press was turned on and the pressure increased to around 1400pa on the dial. The selector was switched from low, middle and high. The cells rise up and then stopped with the top of the press and held on the right pressure and allowing the pressure to build up. The outlet valve was gently opened and the pressure was applied to crush the cells. The sample was then drawn up into the cell. The samples were collected (watch the cells pushed down and quickly switch to the low when reaching the stop mark). This was

repeated three times, and clear cell lysis was obtained. The samples were aliquoted (1ml into 1.5ml tubes), and stored at –80°C.

In vitro AUTOPHOSPHORYLATION AND DE-PHOSPHORYLATION ASSAY

Following expression and lysis by french press, both Ire1p* and Dcr2p were partially purified through TALON Co^{2+} affinity beads (BD Biosciences, CA). The Ire1p* underwent *in vitro* autophosphorylation, then de-phosphorylation by Dcr2p or λ-phosphatase with or without phosphatase cocktail inhibitors (Sigma).

The *in vitro* autophosphorylation of Ire1p* was done as described by Nock et al (Nock et al., 2001). Briefly, Ire1p* was eluted in elution buffer (150mM Imidazole, 300mM NaCl, 50mM Sodium Phosphate). Kinase buffer was added (20mM HEPES (pH 7.5), 10 mM magnesium acetate, 50mM potassium acetate, 1mM DTT), also containing ATP and Aprotinin (1ug/10ul reaction volume). The reactions were incubated at 30°C for 30 min.

De-phosphorylation by either Dcr2p or λ-phosphatase was performed in λ-phosphatase reaction buffer containing 2mM $MnCl_2$ with or without phosphatase cocktail inhibitors I or II from Sigma, and followed by SDS-PAGE protein analysis.

PHOSPHOPROTEIN DETECTION ASSAY

The assay we used (from PIERCE) to detect phosphoproteins was non-radioactive, and relied on chemical modification for the specific detection of phosphorylated proteins. The rationale is the following: PhosphoProbe-HRP is an iron

(Fe^{3+})-activated (or conjugated) derivative of horseradish peroxidase (HRP). PhosphoProbe-HRP exhibits two distinct binding specificities, one of which is phosphate ($R\text{-}PO_3$)-specific. The other binding specificity is related to a carboxyl-containing binding motif that is common to most proteins and some peptides. This carboxyl motif binding specificity can be used in a total protein detection application. However, a novel treatment, reactive chemical blocking (RCB), is used to eliminate this carboxyl-binding motif, thus imparting exclusive specificity toward phosphate groups. PhosphoProbe-HRP, in conjunction with RCB, is a universal phosphate detection probe. PhosphoProbe-HRP has been optimized for direct detection of phosphoester molecules such as nucleotides or protein/peptides containing phosphoserine, phosphothreonine and phosphotyrosine. Basically, the reactive chemical blocking (RCB) uses 1-Ethyl-3-[3-dimethylaminopropyl]carbodiimide hydrochloride (EDC or EDAC) and Ethylaminediamine dihydrochloride (EDA) to modify any carboxyl-group of the protein, consequently blocking its interaction with PhosphoProbe-HRP.

EDC is a zero-length crosslinking agent used to couple carboxyl groups to primary amines. This crosslinker has been used in diverse applications such as forming amide bonds in peptide synthesis, attaching haptens to carrier proteins to form immunogens, labeling nucleic acids through 5' phosphate groups and creating amine-reactive NHS-esters of biomolecules. EDC reacts with a carboxyl to form an amine-reactive *O*-acylisourea intermediate. If this intermediate does not encounter an amine, it will hydrolyze and regenerate the carboxyl group. However, if the amine donor EDA is added into the reaction, carboxylic acids would be covalently modified with

short compounds containing primary amines at either end to form stable amide linkages. This will block the carboxylates and form terminal amino groups.

The procedure is the following: Transfer protein onto nitrocellulose. Include phosphorylated and non-phosphorylated samples for controls. Block the blot with blocking solution (1% BSA) for 1 hour at room temperature with shaking. Wash blot three times with 50 ml of Quench Buffer (0.1 M MES (2-[*N*-morpholino]ethanesulfonic acid), pH 5.0, 50 mM EDA) for 5 minutes each with shaking. Prepare RCB Buffer by adding EDC to a final concentration of 25 mM to the Quench/Wash Buffer. Prepare RCB Buffer immediately before use. Add 50 ml RCB Buffer and shake at room temperature for the optimal time (predetermined from time study). Rinse with 50 ml Quench Buffer followed by two 50 ml washes with Quench Buffer for 5 minutes each. Wash blot three times with 50 ml of Acetate Wash Buffer (0.1 M sodium acetate, 1.0 M NaCl; pH 5.0) for 5 minutes each with shaking. Prepare PhosphoProbe Working Solution by diluting to 5 µg/ml in Acetate Wash Buffer with 0.05% Tween®-20 (a 1:200 dilution of Surfact-Amps 20 results in a final Tween-20 concentration of 0.05%). Remove Acetate Wash Buffer and add PhosphoProbe™ Working Solution (Block buffer). Incubate for 1 hour at room temperature with shaking. Wash four times with 50 ml Acetate Wash Buffer containing 0.05% Tween-20 for 5 minutes each with shaking. Check supernatant of final wash for “free HRP” activity by adding 100 µl of the supernatant to 1 ml of Turbo TMB ELISA substrate. Blue color production within 5 minutes indicates washing was insufficient and requires additional washes. Decant wash solution. Add SuperSignal® Working Solution and incubate without shaking at room

temperature for 5 minutes, then place into plastic sheet protector. Squeeze out excess liquid from the sheet protector by wiping with a paper towel. Ensure that no air bubbles are visible between the sheet protector and the nitrocellulose. Expose to film initially for 1 minute and develop. Blot can be exposed again to film to obtain an optimal image. The same blot can subsequently be blotted with anti-6XHistidine antibody or PAP antibody, to evaluate protein levels of Ire1p* and Dcr2p, respectively.

TCA PROTEIN PRECIPITATION

6ml yeast cultures were grown to mid-log phase. The cells were collected by centrifugation, washed once with distilled water, resuspended in 300ul of 1.85M NaOH with 7% 2-mercaptoethanol and vortexed at high-speed for 1 min. Add 150µl cold 100% Trichloroacetic Acid (TCA) was added and the samples were left on ice for 5min. The cells were centrifuged for 10min at maximum-speed in a microfuge at 4°C. The pellet was washed with 400~500µl 1M Tris-base (un-pHed) and left on ice for 5min. Lastly, the pellet was resuspended in 150µl of 8M Urea Buffer, and stored at –80°C.

PROTEIN ANALYSIS

For co-immunoprecipitation, the cells were lysed using glass beads, and the lysis buffer contained 0.9% NP-40, to extract the transmembrane protein Ire1p. TALON Co^{2+} affinity beads (BD Biosciences, CA) were used to pull down the Dcr2p-TAG (PrA+HA+6XHis) according to their instructions. Briefly, 50µl TALON Co2+ beads

were added; the samples were rotated at 4°C for 2h; washed in extraction buffer for 2 or 3 times; and resuspended in Laemmli buffer with 5% β-mercaptoethanol.

The gels for SDS-PAGE (Laemmli, 1970) contained 8% of a 29:1 acrylamide/bis-acrylamide solution, and transferred onto nitrocellulose. The blots were blocked in PBS containing 5% w/v dry non-fat milk and 0.1% v/v Tween-20. Between incubations the blots were washed three times 10 min each, in PBS.

Protein A fusion proteins were detected with the Peroxidase-Anti-Peroxidase (PAP) soluble complex reagent from Sigma (St. Louis, MO). The blots were processed with chemiluminescent peroxidase reagents from Pierce (Rockford, IL). X-ray films were developed using a Konica QX-130A developer.

PREPARATION OF YEAST RNA

Yeast RNA is efficiently released by disrupting the cells using high-speed mixing in the presence of glass beads and denaturing agents. Proteins are removed by extraction with organic solvents and the RNA is recovered by ethanol precipitation and quantitated by measuring its absorbance at 260 nm. Briefly, approximately 2×10^8 cells were harvested in the mid-log phase, and resuspended in 300µl RNA buffer (0.5M NaCl, 200nM Tris, pH 7.5, 10mM EDTA) and 300µl of 25:24:1 phenol/chloroform/isoamyl alcohol in the presence of 200µl chilled glass beads. They were then vortexed immediately for 2 min at the highest speed. After centrifugation, the aqueous layer was transferred to a clean tube. An equal volume of 25:24:1 phenol/chloroform/isoamyl alcohol was added, and the samples were vortexed for another 10 sec. After

centrifugation, the aqueous layer was collected, and 3 volumes of ice-cold 100% ethanol were added to it. After mixing, the samples were incubated at –20°C for 30 min, and centrifuged for 2min at 4°C. The supernatant was removed and the pellet was washed with ice-cold 70% ethanol. Lastly, the pellet was resuspended in 50µl DEPC-treated H_2O.

NORTHERN ANALYSIS AND RT-PCR

The DNA probe for Northern analysis we used was generated through Biotin Random Prime Kit from PIERCE, from a PCR product corresponding to the gene of interest. The Northern was performed by North2South Chemiluminescent Hybridization and Detection kit from PIERCE. Briefly, the protocol instructions are the following: take the picture of the capillary semi-wet transfer RNA blots and cross-link the blot by UV. Pre-hybridize the blots in Hybridization buffer with rotation for at least 30 min at 65°C. Add the DNA Biotin-labeled probe and hybridize overnight at 45°C. Wash blots three times for 15~20 min per wash with 2X stringency wash buffer (1X buffer contains 2XSSC/0.1% SDS). Add blocking buffer for 15 min at RT and add Streptavidin-HRP for another 15 min at RT. Wash the blots with 1X wash buffer four times for 5 min per wash. Add Substrate Equilibration Buffer for 5 min at RT. Lastly, add North2South Luminol/Enhancer Solution and Stable Peroxide Solution (1:1) for 5 min, expose and develop film.

RT-PCR was performed by Invitrogen kit, according to their instructions, using SuperScript III Reverse Transcriptase and reverse primer for the first cDNA strand, then

regular PCR reaction. Finally analyze through agarose gel electrophoresis and ethidium bromide staining to visualize the products.

TETRAD ANALYSIS

Diploid cells were washed once in 5 ml sterile water. The pellet was resuspended in 2.5 ml SPM buffer (2% potassium acetate), and incubate at room temperature for 5~7 days for sporulation. The cells were examined microscopically for tetrads. 0.5 ml of the sporulation culture were centrifuged, washed in 1 ml water, and resuspended in 50 µl of zymolyase solution (0.5 mg/ml in 1M sorbitol). After an incubation for 8~10 min at 30°C, 0.8 ml sterile water were slowly added to the tube, and placed on ice. 15µl were then plated on a YPD plate, for dissection using a dissection microscope.

SERIAL DILUTION PLATING ASSAY

For examining any growth defect of yeast strains with or without stress, cells were grown into mid-log phase, and the cell density was measured microscopically with a hemacytometer. We used 96-well plates to set up 10 fold serial dilutions, starting at 5000 cells. These numbers of cells were spotted onto plates with a multiple channel pipette.

HIGH THROUGH-PUT YEAST TRANSFORMATION

We used 96 well plates to do transformation of thousands of yeast homozygous diploid knockout strains (~4,300 homozygous deletion strains) by one common plasmid.

The assay was modified from the multiwell transformation protocol used by the Saccharomyces Genome Deletion Project (http://www-sequence.stanford.edu/group/yeast_deletion_project/).

Briefly, we replicated the diploid knockout collection plate to a new plate containing 100µl YPD per well. The plates were incubated overnight, replicated again and incubated overnight at 30°C. The plates were centrifuged at 4000 rpm for 10 min. The media were poured onto a paper tissue inside the hood. We then added 5µl high quality purified plasmid (1~2µg DNA) and 5µl carrier DNA (Salmon Sperm DNA) and 20µl 1X TE/LiAC buffer per well. The plates were incubated at 30°C for 30 min. 150µl 1X TE/LiAC/PEG buffer were added and incubated at 30°C for 30 min. We then added 17µl DMSO, and incubated the plates at 42°C for 15 min. We centrifuged the plates at 4000 rpm for 5 min, removed the transformation mix onto paper tissue inside the hood, added 30µl YPD and incubated the plates at 30°C for 3hrs. Lastly, we spotted the exact layout as the deletion collection plates onto two kinds of 150mm large selective medium plates and incubated them at 30°C for 2~3 days.

CHAPTER III

NUTRIENT-SPECIFIC EFFECTS IN THE COORDINATION OF CELL GROWTH WITH CELL DIVISION IN CONTINUOUS CULTURES OF *Saccharomyces cerevisiae**

INTRODUCTION

When the growth of *Saccharomyces cerevisiae* cells is limited, it is thought that doubling time delays reflect a prolongation of the first gap phase (G1) of the cell cycle, before DNA replication (S phase). Passage through START, a nodal point in late G1 where various aspects of the cell's physiology are monitored, is thought to ensure that growth requirements are met before the cell commits to the process of cell division (Pringle and Hartwell 1981). This general understanding of coordination between growth and division implies that growth control is nutrient-mediated but not nutrient-specific. In other words, as long as two different media compositions allow for the attainment of the same growth rate, the cell cycle profiles of proliferating cells in those two media should be identical. In *S. cerevisiae*, most of the experimental data seem to support the notion that all nutrient limitations exclusively prolong G1 and have very little effect on the

---

*Reprinted with permission from "Nutrient-specific effects in the coordination of cell growth with cell division in continuous cultures of *saccharomyces cerevisiae*" by Guo, J., Bryan, B. A., and Polymenis, M., (2004), Arch Microbiol *182*, 326-330. Copyright 2004 by Springer with kind permission of Springer Science and Business Media.

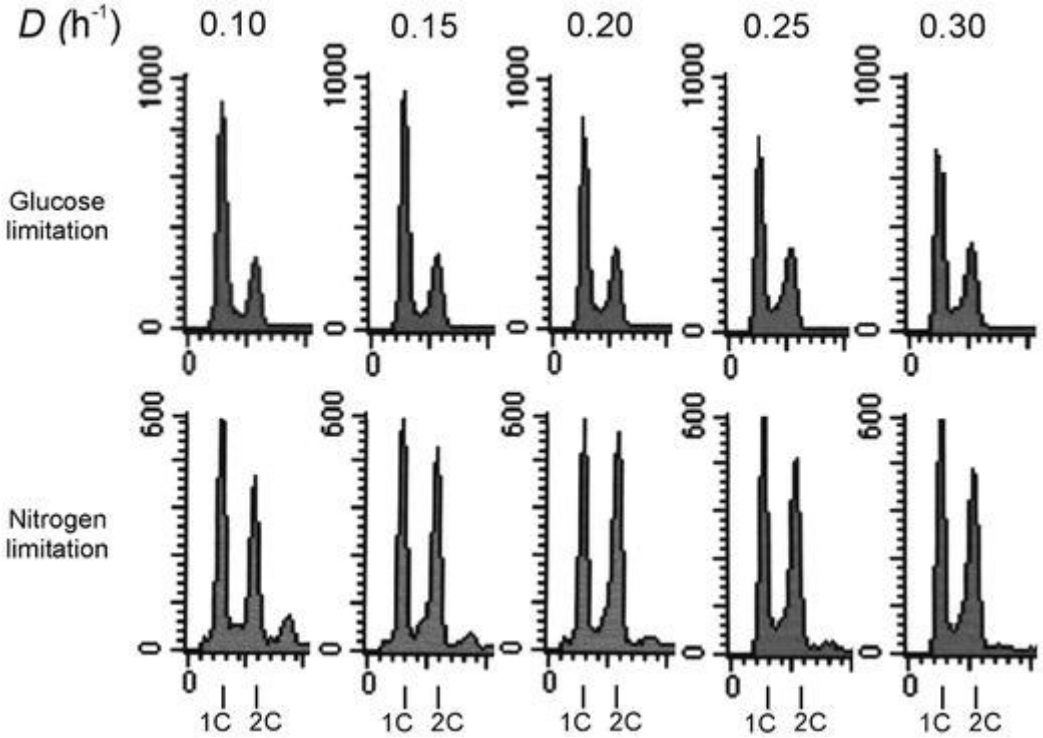

Figure 3.1 Cell cycle progression at different growth rates and nutrient limitations. The cellular DNA content of *Saccharomyces cerevisiae* haploid strain BY4741 grown in chemostats at the indicated dilution rate and nutrient limitation was determined by flow cytometry. The *y*-axis represents the number of cells analyzed and the *x*-axis represents fluorescence per cell. The DNA content of cells in G1 and G2/M is indicated as 1C (the first peak) and 2C (the second peak), respectively. The DNA content panels shown are from Experiment 1 of Table 3.1.

other phases of the cell cycle (Pringle and Hartwell 1981). But in the vast majority of previous studies, alterations in growth rate were inseparable from nutrient-specific variables. To our knowledge, a comparison of cell cycle profiles, using accurate modern methodologies, in different nutrients and growth rates in continuous steady-state cultures is lacking.

RESULTS

Haploid strain BY4741 strain growing under either glucose or nitrogen limitation was examined at five different growth rates in each case, from 0.3 h^{-1} (2.31 h generation time) to 0.1 h^{-1} (6.93 h generation time). For each nutrient limitation two separate chemostat experiments were performed. At all growth rates and nutrient limitations, about 90% of cells were able to form colonies on solid media, suggesting that there were no growth rate or nutrient-specific effects on cell viability (data not shown).

As glucose-limited cultures proliferated more slowly, the duration of the G1 phase linearly increased from 43% (at D=0.3 h^{-1}) to 63% (at D=0.1 h^{-1}) of the total generation time (Figure 3.1, Table 3.1). In absolute terms this reflects a 4.4-fold increase (from 1 h to 4.4 h), even though the growth rate difference was 3-fold. The non-G1 phases progressively expanded too, but to a lesser extent (from 1.3 h to 2.6 h; Figure 3.1, Table 3.1). It has been reported that in glucose-limited chemostats and for growth rates as low as 0.08 h^{-1} there is no increase in the duration of the cell cycle phases after initiation of DNA replication (Carter and Jagadish, 1978), and non-G1 phase expansion is detectable only at lower growth rates (Carter and Jagadish, 1978; Jagadish and Carter,

1977). The chemostat media used in these older studies contained much higher amounts of glucose (10 g/l) than in our study (0.8 g/l) and they were also complex, containing peptone and yeast extract (Carter and Jagadish, 1978; Jagadish and Carter, 1977; Johnston et al., 1979). We used minimal defined media (see above) to properly separate nutrient-specific from growth rate-specific variables. We also used different strains and in the older experiments (Carter and Jagadish, 1978; Jagadish and Carter, 1977; Johnston et al., 1979) chemostats were run at 24°C vs 30°C in our case. Perhaps more importantly, at the time of these older studies flow cytometry was not available and the duration of cell cycle phases was indirectly deduced using conditional cell division cycle (cdc) mutants, which require temperature and media changes (Jagadish and Carter 1977; Carter and Jagadish 1978; Pringle and Hartwell 1981). These experimental protocols perturb steady-state conditions of cell proliferation and introduce an additional level of uncertainty in the analysis and interpretation of the relevant data. It was later shown that these cdc strains are unreliable indicators of cell cycle parameters due to variability in the execution point (Richmond and Williamson, 1983). The above differences between the older studies and ours could account for the discrepancy in the obtained results.

Table 3.1 Cell size and G1 length of the haploid BY4741 *Saccharomyces cerevisiae* strain at different growth rates and nutrient limitations. For every reported value, the chemostats were sampled three times, of which the average and standard deviation is shown in each case

D (h^{-1})	Measured parameter	Glucose limitation		Nitrogen limitation	
		Experiment 1	Experiment 2	Experiment 1	Experiment 2
0.1	% in G1	61.3±0.3	63.1±0.6	40.0±0.4	46.0±1.0
	Cell size (μm^3)	19.3±0.2	19.1±0.2	33.8±0.3	32.5±0.2
	Cell density (10^7 cells/ml)	5.7±0.1	5.6±0.1	5.5±0.1	5.9±0.2
0.15	% in G1	57.7±0.6	57.4±0.5	40.3±0.7	44.6±1.0
	Cell size (μm^3)	18.4±0.2	19.2±0.3	29.6±0.1	29.5±0.3
	Cell density (10^7 cells/ml)	5.6±0.1	5.3±0.02	4.9±0.1	4.6±0.2
0.20	% in G1	52.1±0.4	49.7±0.5	34.4±0.3	40.3±0.9
	Cell size (μm^3)	18.1±0.6	17.6±0.1	28.8±0.1	29.8±1.0
	Cell density (10^7 cells/ml)	5.2±0.04	4.1±0.1	2.6±0.2	3.6±0.1
0.25	% in G1	48.3±0.4	46.9±0.8	38.7±0.7	37.0±0.5
	Cell size (μm^3)	19.0±0.2	19.0±0.4	28.9±0.2	30.9±0.3
	Cell density (10^7 cells/ml)	4.4±0.1	3.4±0.1	1.4±0.1	2.8±0.1
0.30	% in G1	44.0±0.6	42.8±0.6	41.5±0.3	41.2±0.3
	Cell size (μm^3)	18.4±0.1	19.4±0.5	30.9±0.1	29.1±0.1
	Cell density (10^7 cells/ml)	2.4±0.1	1.9±0.1	0.5±0.02	0.7±0.02

Cell numbers and the mean cell volume of live unfixed samples were also measured. Cell size remained constant at all growth rates tested (Table 3.1). This has been seen before for glucose-limited chemostat cultures with growth rates lower than 0.23 h^{-1} (Johnston et al., 1979), although in that study it was also reported that cell size increased by about 30% when growth rate increased to 0.31 h^{-1}. Another difference between our study and that of Johnston et al. (1979) is that the mean cell size was significantly smaller (by about 50%) under our conditions, reaching 19 μm^3 on average, which probably reflects the differences outlined above in media and/or strain background between that study and ours.

In nitrogen-limited cultures, there was a proportional prolongation of G1 and non-G1 phases (Figure 3.1, Table 3.1). G1 reproducibly occupied about 40% of the total generation time at all growth rates tested (Figure 3.1, Table 3.1). Given the prevailing views mentioned above, we were surprised by the fact that G1 expansion did not primarily account for the increase in the generation time. Cell size also remained constant as a function of growth rate (Table 3.1). Nitrogen-limited cells were larger than

glucose-limited cells proliferating at the same rate, consistent with earlier observations by Adams (1977). In nitrogen-limited cultures and at low dilution rates (0.1 h^{-1} and 0.15 h^{-1}), a small fraction (<5% of total) of cells had a 3C DNA content (Figure 3.1). The cells in that fraction were not included in the calculations of the percent of cells in G1 shown in Tables 3.1 and 3.2. Note, however, that if one includes this population in the calculations, then the fraction of G1 cells would be even lower than the estimates we present, further strengthening our conclusions. Finally, the prototrophic strain X2180-5B was also examined. In that case too, non-G1 cell cycle phases expanded during nitrogen limitation (Table 3.2). Thus, auxotrophic supplements do not appear to influence the results. Under nitrogen limitation, cells with a 3N DNA content were also present at a dilution rate of 0.1 h^{-1} but they were barely detectable at 0.15 h^{-1} (not shown). Therefore, the appearance of 3C cells at low growth rates during nitrogen limitation is probably not strain-specific, although their relative abundance may vary among different strain backgrounds.

Table 3.2 Cell size and G1 length of the prototrophic haploid X2180-5B *S. cerevisiae* strain at different growth rates during nitrogen limitation. For every reported value, the chemostats were sampled three times, of which the average and standard deviation is shown in each case.

D (h^{-1})	Measured parameter	Experiment 1	Experiment 2
0.1	% in G1	47.6±1.9	45.1±1.2
	Cell size (μm^3)	24.5±0.2	25.0±0.3
	Cell density (10^8 cells/ml)	1.4±0.1	1.4±0.04
0.15	% in G1	49.1±0.9	47.0±0.8
	Cell size (μm^3)	21.7±0.3	22.4±0.1
	Cell density (10^8 cells/ml)	1.3±0.1	1.4±0.1
0.20	% in G1	43.0±0.1	42.9±0.4
	Cell size (μm^3)	21.0±0.4	22.0±0.3
	Cell density (10^8 cells/ml)	1.2±0.02	1.1±0.1
0.25	% in G1	41.1±0.5	41.1±0.9
	Cell size (μm^3)	21.9±0.1	21.9±0.4
	Cell density (10^8 cells/ml)	0.9±0.01	0.8±0.04
0.30	% in G1	42.1±0.2	41.4±0.4
	Cell size (μm^3)	22.4±0.1	22.4±0.04
	Cell density (10^8 cells/ml)	0.6±0.03	0.5±0.02

Cell cycle progression under the above conditions was also evaluated by microscopic examination of bud formation and nuclear morphology (Figure 3.2). Cells with one nucleus were classified as unbudded, small budded (when the fraction of the diameter of the bud compared to the mother cell was equal or less than 0.4), and large budded (when the relative bud diameter was higher than 0.4). The percentage of cells with a dividing (in anaphase) or fully divided (in telophase) nucleus was also measured. These experiments confirmed the general conclusion of the DNA content data, because the percentage of unbudded cells (indicative of the length of the G1 phase) was in very good agreement with the results of the DNA content measurements (Table 3.1). Interestingly, however, it appears that, compared to glucose limitation, nitrogen-limited cells spent more time in late stages of the cell cycle, especially in mitosis (Figure 3.2).

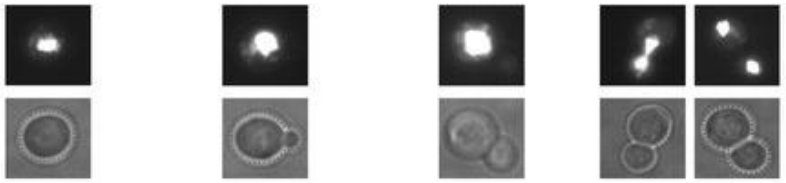

	$D(h^{-1})$	I	II	III	IVa+IVb
Glc-limited	**0.10** (n=452)	69	10	6	15
	0.15 (n=470)	61	12	15	12
	0.20 (n=418)	56	14	18	12
	0.25 (n=375)	47	20	15	18
	0.30 (n=357)	42	22	19	17
N-limited	**0.10** (n=402)	42	18	11	29
	0.15 (n=396)	45	26	12	17
	0.20 (n=404)	47	24	16	13
	0.25 (n=392)	43	25	14	18
	0.30 (n=476)	47	23	10	20

Figure 3.2 Cell and nuclear morphology as a function of growth rate under glucose (Glc) or nitrogen (N) limitation. The number of cells evaluated for each dilution rate and nutrient limitation is shown in *parentheses*. The strain used was the same as in Figure 3.1 (haploid BY4741 background). The cells were grouped in four different classes (I–IV). The fourth class was composed of cells in anaphase (IVa) and telophase (IVb). Representative photographs for each class are shown on *top*, taken from nitrogen-limited cells. The *top panels* display the nuclear morphology for each class evaluated by fluorescence microscopy, while the *bottom panels* display the overall cell morphology evaluated by phase microscopy. The percentage of cells in each class is shown below the corresponding panels. (The unbudded cell group corresponds to G1 phase cells)

DISCUSSION

Experiments aimed at separating nutrient-specific from growth rate-specific parameters during steady-state growth were carried out and cell cycle progression was evaluated using modern accurate methods. We are not aware of an analogous study in *S. cerevisiae* that directly compared cell cycle profiles in nitrogen-limited versus glucose-limited chemostats.

The differences between glucose and nitrogen limitation (Table 3.1) argue for nutrient-specific effects on cell cycle progression, independent of growth rate per se. While glucose is mainly used for energy production, nitrogen's role is exclusively anabolic. Interestingly, reserve carbohydrate metabolism has been recently linked to the duration of the G1 phase in continuous cultures (Paalman et al., 2003). Overall, it is unlikely that our results reflect "anomalies" peculiar to chemostat cultures. In any case, it is clear that glucose and nitrogen limitation differentially affect the length of the G1 phase. Perhaps the term "cell growth" is too general and does not accurately describe the interplay between distinct metabolic processes and cell division.

Our results are not adequately accommodated by current ideas about how cell growth is coordinated with cell division. There is no question that upon starvation cells +exit the cell cycle and arrest in G1 (or G0). This situation, however, may not extend to continuously dividing cell populations. The notion that all metabolic pathways are somehow collectively "sensed" only in G1 prior to START is very useful conceptually, but it might be an oversimplification. It should not be surprising that the duration of cell cycle phases is not fixed, but instead varies upon different nutrient and growth rate

limitations. This is also reflected in the different "growth" requirements for cell division manifest among different organisms, including other fungi such as *Schizosaccharomyces pombe* and *Neurospora crassa* (Griffin, 1994). For example, in *S. pombe*, a G1 growth requirement is also present, but it remains cryptic because in this organism the G2/M transition is very sensitive to overall cell growth (Nasmyth, 1979). Although under nitrogen-limited chemostat conditions an exclusive G1 prolongation was observed in *S. pombe* cells (Nasmyth 1979), the different cell cycle phases were determined indirectly using *cdc* mutants, which were later shown to provide inaccurate estimates (Richmond and Williamson, 1983).

Finally, several mutations are known to change the duration of individual cell cycle phases with negligible effects on the overall doubling time, because there are compensatory changes in other phases (Neufeld and Edgar, 1998; Polymenis and Schmidt, 1999). Variability in the duration of cell cycle phases probably allows for a better adjustment to different environments, which might impose different metabolic needs.

CHAPTER IV

THE Dcr2p PHOSPHATASE TARGETS Ire1p AND DOWNREGULATES THE UNFOLDED PROTEIN RESPONSE IN *Saccharomyces cerevisiae**

INTRODUCTION

The unfolded protein response (UPR) is triggered when protein synthesis exceeds the protein folding capacity of the cell, and also by acute 'environmental' stresses, such as exposure to tunicamycin or dithiothreitol, which block glycosylation or disulfide bond formation, respectively (Kaufman et al., 2002; Schroder et al., 2000). In yeast, inositol requirement 1 (Ire1p), an endoplasmic reticulum transmembrane protein with its amino-terminal domain located in the lumen of the endoplasmic reticulum, senses unfolded proteins (Patil and Walter, 2001; Rutkowski and Kaufman, 2004). Ire1p has kinase and endonuclease activities, which reside in distinct cytosolic domains. When Ire1p dimerizes, it is autophosphorylated *in trans*, primarily on Ser 840 and Ser 841, followed by activation of its endonuclease activity towards its sole substrate, the homologous to Atf/Creb1 (*HAC1*) messenger RNA (Niwa et al., 2005; Patil and Walter, 2001).

---

*Reprinted from "Dcr2 targets Ire1 and downregulates the unfolded protein response in *Saccharomyces cerevisiae*" by Guo, J., and Polymenis, M., 2006, EMBO Report, *7*, 1124-7, Copyright 2006 by European Molecular Biology Organization.

If Ser 840 and Ser 841 cannot be phosphorylated, for example, in Ire1p-S840A, S841A, UPR signaling is essentially eliminated (Shamu and Walter, 1996).

When the UPR is not induced, the *HAC1*^{u} transcript is stable in the cytosol but is not translated efficiently because an intron blocks its translation (Patil and Walter, 2001; Rutkowski and Kaufman, 2004). Active Ire1p cleaves *HAC1*^{u} mRNA at two splice sites removing the intron, and the two exons are ligated by transfer RNA ligase, generating *HAC1*^{i} mRNA (Sidrauski et al., 1996; Sidrauski and Walter, 1997). *HAC1*^{i} is then translated efficiently and Hac1p^{i} activates transcription of approximately 300 UPR target genes (Patil & Walter, 2001; Rutkowski & Kaufman, 2004). In addition to regulated *HAC1* mRNA splicing, which is Ire1p dependent. *HAC1* mRNA transcription is also regulated through an Ire1p-independent pathway (Leber et al., 2004).

The UPR is anti-mitogenic. Constitutive expression of the intron-less *HAC1*^{i} transcript inhibits cell proliferation in yeast (Kawahara et al., 1997). In mammalian cells, the UPR modulates apoptosis and also delays cell-cycle progression (Brewer and Diehl, 2000; Brewer et al., 1999). How the UPR is activated is fairly well established, but it is not yet clear how it is downregulated. Given the anti-mitogenic properties of the UPR, a mechanism that turns off the UPR must exist.

We had previously identified the dose-dependent cell-cycle regulator 2 (Dcr2p) phosphatase on the basis of its positive role in cell-cycle progression (Pathak et al., 2004). Here we show that Dcr2p interacts with Ire1p functionally and physically, both *in vitro* and *in vivo*, and that Dcr2p acts antagonistically to the UPR.

RESULTS

A genome-wide screen to identify cellular roles for Dcr2p. From a genetic screen for gene products that alter the timing of START (Bogomolnaya et al., 2004a), we found that over-expression of the uncharacterized ORF *YLR361C* accelerates initiation of DNA replication, while its deletion delays START completion (Pathak et al., 2004). Consequently, we named *YLR361C DCR2* (Dosage-dependent Cell Cycle Regulator 2). The *DCR2* ORF is predicted to encode a 578 amino acid protein similar to phosphoesterases, which are present in all organisms (Pathak et al., 2004). The phosphatase domain of Dcr2p occupies the C-terminal half of the protein (positions 244-566). The N-terminal half of Dcr2p has no similarity to any proteins in the database.

We had previously generated a dominant-negative *DCR2* allele, by introducing an H338A substitution (Pathak et al., 2004). This single amino acid change in other phosphatases blocks hydrolysis, but allows substrate binding (Zhuo et al., 1994). Cells carrying the *DCR2-H338A* dominant-negative allele have significantly diminished Dcr2p function, based on the ability of this allele to block START acceleration by the wild type *DCR2* allele (Pathak et al., 2004).

To determine cellular roles of Dcr2p, we sought to identify genes that when deleted in combination with *DCR2* lead to synthetic growth defects. We screened the homozygous diploid yeast deletion panel by introducing with rapid 96-well format transformations a galactose-inducible *DCR2-H338A* allele on a plasmid. We then looked for synthetic growth defects in galactose-containing media, in which *DCR2-H338A* expression is in.duced, compared to glucose-containing media when its expression is

repressed (Figure 4.1A). In wild type cells, over-expression of the *DCR2-H338A* allele does not significantly affect overall cell proliferation (Figure 4.1B). Growth of each strain carrying the galactose-inducible *DCR2-H338A* allele was compared to empty-vector control transformants. In this manner, we interrogated 4,021 deletion strains, of which 221 initially appeared to proliferate slower in the presence of galactose. Upon re-examination, we identified 12 deletion strains that displayed a ≥10-fold growth defect when *DCR2-H338A* expression was induced (Figure 4.1B).

A previous large-scale study reported synthetic interactions between *DCR2* and *RIC1* or *YPT6* (Tong et al., 2001). Ric1p acts as a GTP exchange factor for the Ypt6p GTPase, regulating intracellular trafficking (Siniossoglou et al., 2000). We confirmed these interactions, and identified additional ones involving mostly gene products with trafficking roles (Figure 4.2 and 4.1B). We included in this group the uncharacterized ORF *YKL091C* (*SFH1*), which encodes a Sec14p-like polypeptide. The functional significance of the interactions with Img2p (involved in mitochondrial protein synthesis), Rai1p (involved in rRNA processing) and Tna1p (a nicotinamide transporter) is unclear. Finally, since we used a dominant-negative allele for our analysis (Figure 4.1A), it is possible that the results we obtained underestimate the extent of genetic interactions involving *DCR2*. This might explain why Tong et al. found that double *dcr2Δ, ric1Δ* cells are inviable (Tong et al., 2001), as opposed to slow growing in our analysis (Figure 4.1B).

Figure 4.1 A genome-wide screen to identify cellular roles for Dcr2p. (A) Schematic representation of a systematic introduction of a dominant-negative *DCR2* allele (*GAL-DCR2*^{DN}) into yeast deletion strains and of expected phenotypes. (B) Synthetic growth defects of deletion strains when expression of the *DCR2*^{DN} allele was induced. Growth of the strains (all in the diploid BY4743 (BY4741/BY4742) background) carrying the indicated plasmids was evaluated by spotting 10-fold serial dilutions of the cultures on solid glucose- (Glc) or galactose-containing (Gal) synthetic complete (SC) media. The plates were incubated at 30°C and photographed after 2 (Glc) or 4 (Gal) days.

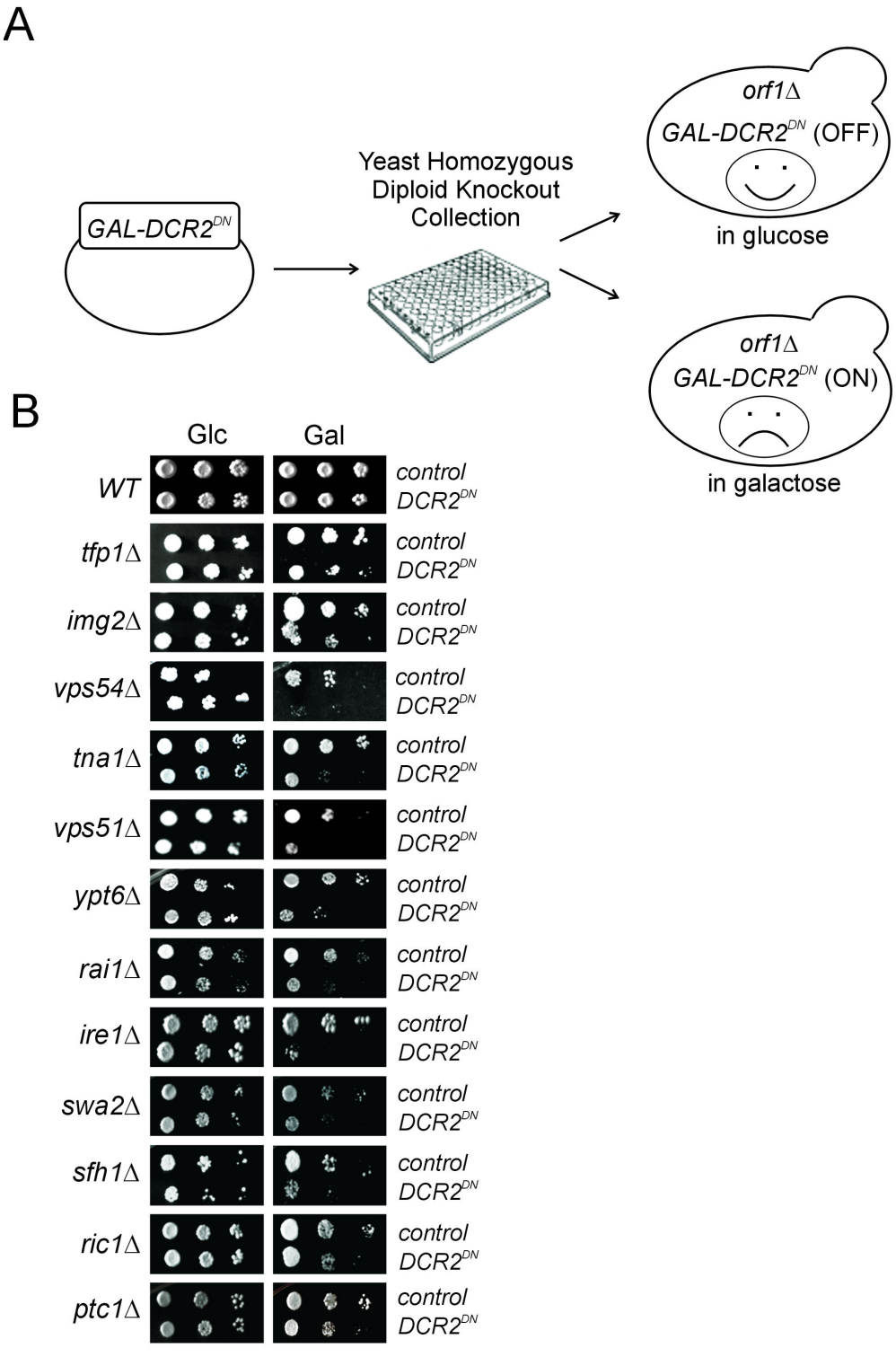
A
GAL-DCR2DN
Yeast Homozygous Diploid Knockout Collection
orf1Δ
GAL-DCR2DN (OFF)
in glucose
orf1Δ
GAL-DCR2DN (ON)
in galactose
B
Glc
Gal
WT
tfp1Δ
img2Δ
vps54Δ
tna1Δ
vps51Δ
ypt6Δ
rai1Δ
ire1Δ
swa2Δ
sfh1Δ
ric1Δ
ptc1Δ
control
DCR2DN

Dcr2p antagonizes the unfolded protein response. In a genome-wide screen to identify genetic interactions involving *DCR2* (see previous section), we found that *ire1Δ* cells carrying a dominant-negative *DCR2* allele grow poorly (Figure 4.1). Furthermore, most of the gene products that showed genetic interactions with *DCR2* had some role in trafficking (Figure 4.2). Because defects in transportation trigger the UPR (Patil and Walter, 2001), thereby possibly explaining our findings, we examined the functional interactions between *DCR2* and *IRE1*. First, we deleted both *DCR2* and *IRE1* and found that *dcr2Δ*, *ire1Δ* double mutants grow extremely poorly (Figure 4.3A). We then artificially triggered the UPR, by blocking glycosylation with tunicamycin, and examined cell proliferation (Figure 4.3B). Under these conditions, loss of *IRE1* is lethal (Figure 4.3B). It seems that altering the dosage of *DCR2* impairs viability in the presence of tunicamycin, although not to the same extent as *ire1Δ* cells (Figure 4.3B).

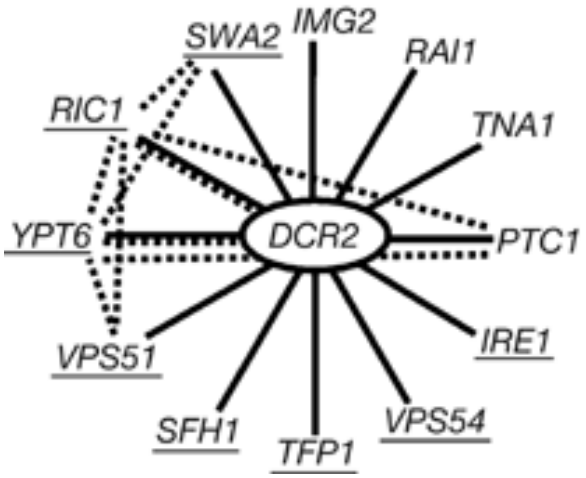

Figure 4.2 Genetic interactions of *DCR2*. Solid lines indicate interactions identified in this study, and dotted lines represent interactions reported previously (Tong *et al*, 2001). Open reading frames with a role in trafficking, on the basis of the annotations of the Saccharomyces Genome Database, are underlined.

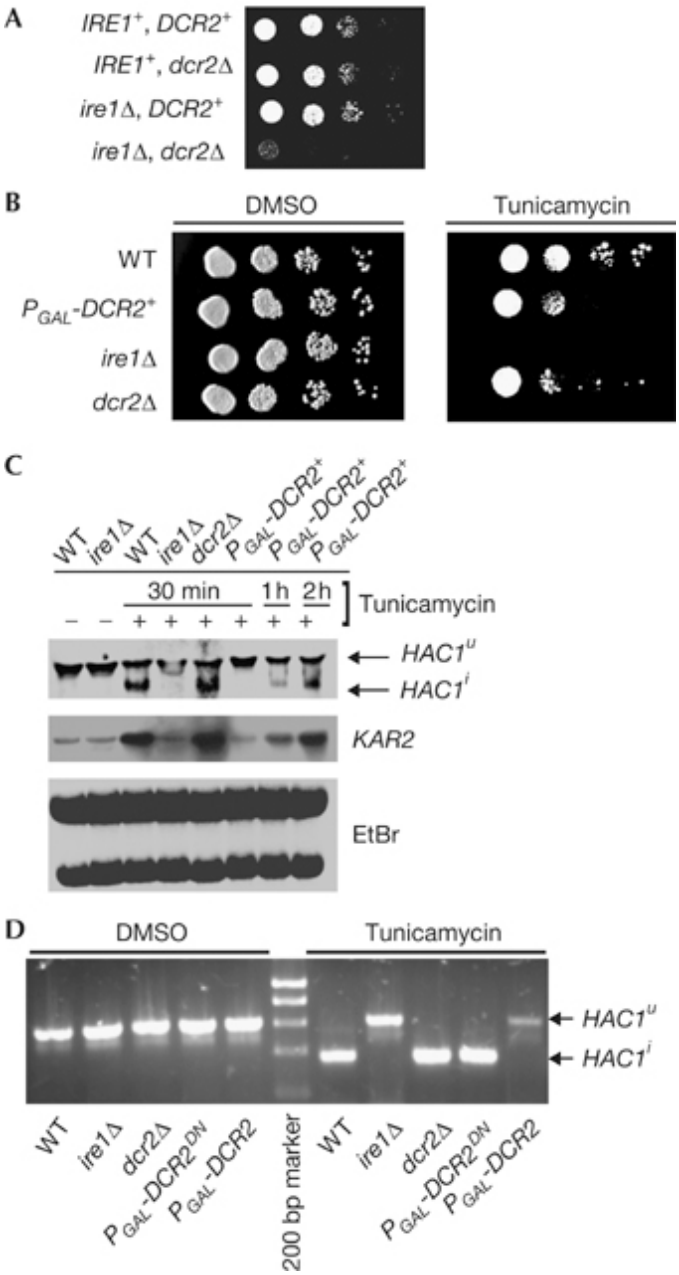

Figure 4.3 Unfolded protein response signaling is sensitized in *DCR2* mutants. (A) Synthetic growth defects of the indicated strains (all in the BY4741 background) were evaluated by spotting ten-fold serial dilutions of the cultures on standard (YPD) medium. The plates were incubated at 30°C and photographed after 2 days. (B) Growth of the indicated strains (all in the BY4741 background) was evaluated on solid galactose medium, containing tunicamycin or DMSO alone. The plates were incubated at 30°C and photographed after 4 days. (C) Steady-state levels of *HAC1* and *KAR2* RNA are shown on an RNA blot. Each lane was loaded with total RNA prepared from the indicated strains (all in the BY4741 background). The ethidium bromide (EtBr)-stained gel is shown at the bottom, to indicate loading. (D) The indicated strains (all in the BY4743 background) were grown in galactose-containing medium in the presence of tunicamycin or DMSO alone, for 30 min. Cells marked as P_{GAL}-*DCR2*^{DN} or P_{GAL}-*DCR2* were carrying the corresponding plasmids, but were otherwise wild type. RNA was extracted and transcription–PCR products with *HAC1*-specific primers were resolved by agarose gel electrophoresis and visualized with EtBr. WT, wild type.

We then examined splicing of HAC1 mRNA, which provides an unambiguous molecular metric of Ire1p activation (Niwa et al., 2005). If Dcr2p interferes with UPR signaling, the relative levels of the unspliced *HAC1*^{u} versus the spliced *HAC1*^{i} mRNA should change in *DCR2* mutants. We monitored *HAC1* splicing by RNA blotting (Figure 4.3C) and reverse transcription–PCR (RT–PCR; Figure 4.3D). When we introduced endoplasmic reticulum stress, by the addition of tunicamycin for 30 min, splicing of *HAC1* was inhibited in cells overexpressing *DCR2* (Figure 4.3C,D), but not the catalytically inactive *DCR2*^{DN} allele (Figure 4.3D). After prolonged incubation (2 h) with tunicamycin, *HAC1*^{u} mRNA was eventually spliced in cells overexpressing *DCR2* (Figure 4.3C). We confirmed UPR induction by monitoring the mRNA levels of karyogamy 2 (*KAR2*), a UPR-responsive gene (Figure 4.2C). Our observations suggest that the Dcr2p phosphatase antagonizes the UPR at a step preceding *HAC1*^{u} mRNA splicing.

Dcr2p de-phosphorylates Ire1p. We examined whether Ire1p interacts physically with Dcr2p. Ire1p, when activated, is autophosphorylated at Ser 840 and Ser 841 (Shamu and Walter, 1996). We constructed strains carrying as their sole *IRE1* copy *IRE1-S840E, S841E* or *IRE1-S840A, S841A* mutant alleles, which mimic or abolish phosphorylation, respectively. The viability of cells carrying either of these alleles is decreased in conditions that trigger the UPR, especially for *IRE1-S840A, S841A* cells (Figure 4.4A), suggesting that reversible phosphorylation of Ire1p is important for proper UPR signaling.

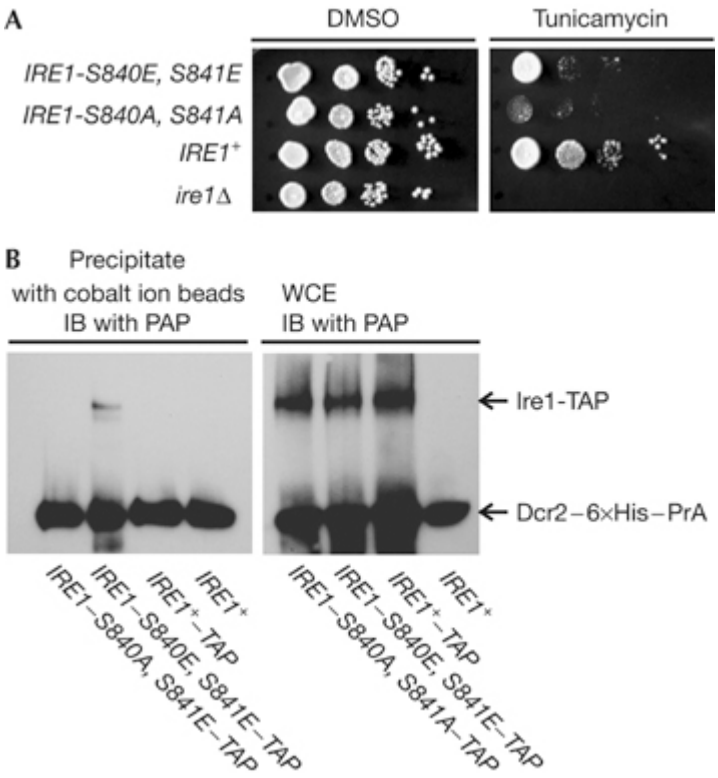

Figure 4.4 Dcr2p physically interacts with Ire1p *in vivo*. (A) Growth of the indicated strains carrying Ser 840 and Ser 841 substitutions (all in the BY4741 background) was evaluated on solid glucose medium. All the *IRE1* alleles were tagged at their carboxyl terminus with the tandem affinity purification (TAP) epitope. The plates were incubated at 30°C and photographed after 2 days. (B) Whole-cell extracts (WCE) from the indicated strains were subjected to SDS–polyacrylamide gel electrophoresis either directly (right) or after Dcr2p was precipitated with cobalt ion beads (left). For immunoblotting (IB), we used the peroxidase–anti-peroxidase (PAP) reagent, which recognizes the protein A (PrA)-tagged Ire1p and Dcr2p.

We then examined whether Dcr2p interacts physically *in vivo* with mutant or wild-type Ire1p (Figure 4.4B). For this experiment, *DCR2* was epitope tagged at its carboxyl terminus with the 'TAG' epitope (6×His, haemagglutinin, protein A) and it was expressed from a galactose-inducible promoter (Gelperin et al., 2005). *IRE1* and the mutant *IRE1* alleles were expressed as C-terminal fusions with the 'TAP' epitope (calmodulin-binding protein, protein A) from its chromosomal location (Ghaemmaghami et al., 2003). From these cells, we used cobalt ion beads to precipitate Dcr2p (through the 6×His epitope), and we noticed that Ire1p-S840E,S841E co-precipitated with Dcr2p (Figure 4.4B). We did not observe interactions between Dcr2p and wild-type Ire1p or Ire1p-S840A,S841A, suggesting that the glutamic acid (E) substitutions allow stable (and detectable) interactions with Dcr2p. These results indicate that Dcr2p interacts physically with Ire1p *in vivo*, and that this interaction is dependent on the phosphorylation status of Ire1p at Ser 840 and Ser 841.

We also examined whether recombinant Dcr2p from bacteria can de-phosphorylate recombinant Ire1p. For this experiment, we expressed in bacteria the cytosolic portion of Ire1p (Ire1p*), which was purified and autophosphorylated (Papa et al., 2003). In the presence of recombinant Dcr2p, Ire1p* was de-phosphorylated, but not when phosphatase activity was blocked (Figure 4.5A). Complete de-phosphorylation of Ire1p by Dcr2p would not be expected because some phosphates might be on sites not targeted by Dcr2p. Our results are consistent with the idea that Ire1p is a substrate for Dcr2p.

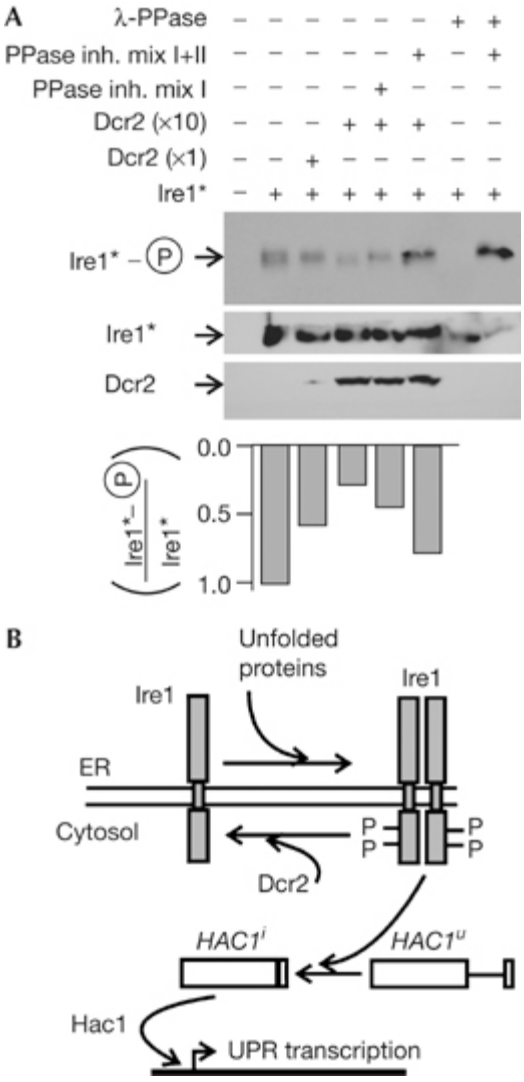

Figure 4.5 Dcr2p de-phosphorylates Ire1p *in vitro*. (A) Recombinant autophosphorylated Ire1p* was incubated with recombinant Dcr2p (the ×1 and ×10 designations refer to the relative amount of Dcr2p added to the reactions) or λ-protein phosphatase (λ-PPase), in the presence (+) or absence (-) of phosphatase inhibitor (PPase inh.) cocktails (cocktail I alone, or I+II), as indicated. The reactions were analyzed by SDS–polyacrylamide gel electrophoresis and blotting, followed by phosphoprotein-specific detection (top), immunoblotting with a 6×His antibody (middle) or immunoblotting with the peroxidase–anti-peroxidase reagent (bottom). The relative amounts of phosphorylated Ire1p* detected are shown on the chart below; they were calculated from the relevant band intensities. (B) A schematic model of the role of Dcr2p as an unfolded protein response (UPR) antagonist, acting on Ire1p and before *HAC1^{u}* splicing. ER, endoplasmic reticulum.

DISCUSSION

Here, we present experiments that link the Dcr2p phosphatase with Ire1p and the UPR. We had originally identified Dcr2p for its pro-mitogenic properties when it is overexpressed (Pathak et al., 2004). This could perhaps be accounted for by Dcr2p acting as an Ire1p phosphatase, as endoplasmic reticulum stress arrests the cell cycle and the UPR is sensitive to nutrients (Kaufman et al., 2002; Schroder et al., 2000) and ATP levels (Papa et al., 2003). However, if Dcr2p acted solely on Ire1p to affect cell proliferation, cells lacking both *IRE1* and *DCR2* should proliferate as fast as those lacking *IRE1* or *DCR2* alone (Figure 4.3A). It is likely that Dcr2p also has an impact on overall cell proliferation independent of Ire1p (Pathak et al., 2004; Pathak, R., Guo, J., Blank, H.M. and Polymenis, M., unpublished data).

How important is the role of Dcr2p in downregulating UPR signaling? Given the functional interactions between *DCR2* and genes involved in trafficking in general (Figure 4.2)—and *IRE1* in particular (Figure 4.3)—as well as the physical interactions between Dcr2p and Ire1p (Figure 4.4, Figure 4.5), it is reasonable to conclude that Dcr2p has a significant role in the UPR. This role of Dcr2p is probably shared with other phosphatases. Although loss of Dcr2 alone only weakly sensitizes cells to endoplasmic reticulum stress (Figure 4.3B; Figure 4.6), the combined loss of Dcr2p and protein phosphatase type 2C (Ptc1p) leads to markedly reduced viability (Figure 4.6B). Another phosphatase, Ptc2p, was also previously shown to de-phosphorylate Ire1 in vitro (Welihinda et al., 1998), and over-expression of *PTC2* downregulated the UPR (Welihinda et al., 1998). It is important to note, however, that Ptc2p and Ire1p have not

been shown to associate *in vivo* and genetic interactions of *PTC2* with *IRE1* or any other gene involved in secretion and/or transportation have not been reported. Finally, although Dcr2p levels are not affected by the UPR, Dcr2p seems to be post-translationally modified when the UPR is triggered (Figure 4.7), indicating some kind of feedback control. Overall, it is clear that de-phosphorylation of Ire1p provides a mechanism for turning off the UPR after it is activated (Figure 4.5B). Other mechanisms that downregulate the UPR in yeast must certainly exist, especially because Ire1p-independent pathways also contribute to UPR signaling (Leber et al., 2004; Schroder et al., 2003).

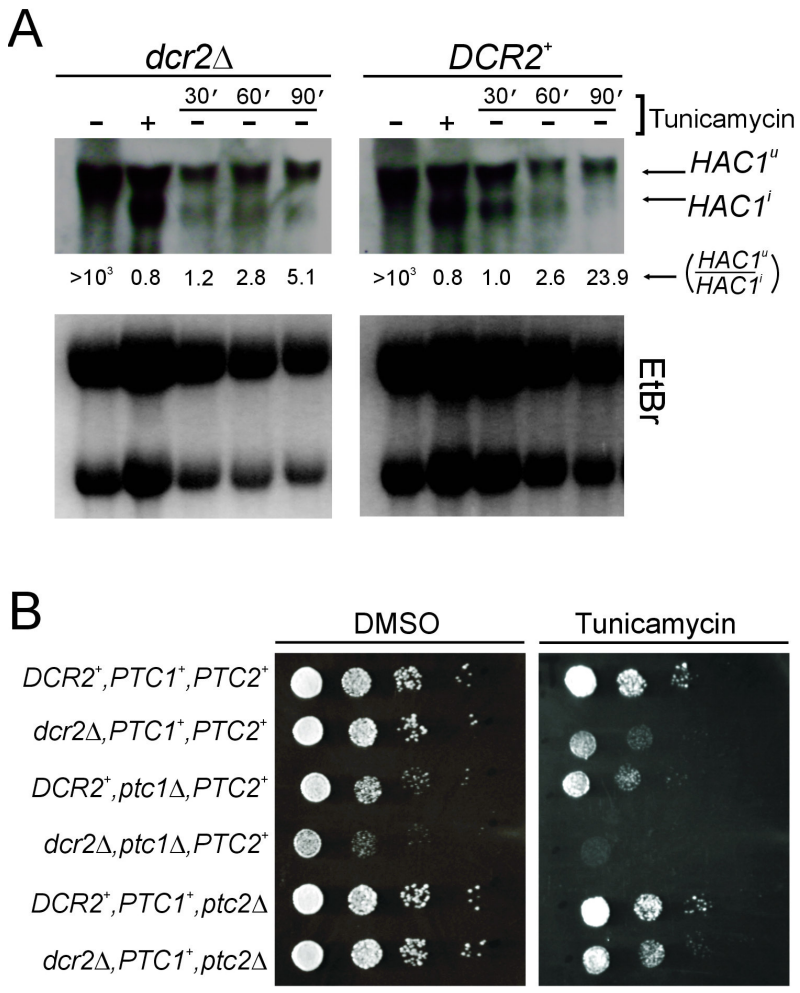

Figure 4.6 *HAC1* splicing recovery in *DCR2* mutants and genetic interaction between *DCR2* and *PTC1*. (A) Cells lacking *DCR2* recover from ER stress with near-normal kinetics. Steady-state levels of *HAC1* were evaluated as in Figure 2C. Where indicated, cells were treated with tunicamycin for 1h, and then grown in drug-free medium for the indicated time. The relative ratio of the unspliced (*HAC1u*) vs. the spliced (*HAC1i*) form of *HAC1* is shown at the bottom of the *HAC1* blots, from the intensity of the relevant bands. (B) Genetic interactions involving *DCR2*, *PTC1* and *PTC2*. Growth of the indicated strains (all in the BY4741 background) was evaluated by spotting 10-fold serial dilutions of the cultures on solid galactose medium, containing tunicamycin or DMSO alone. The plates were incubated at 30°C and photographed after 4 days.

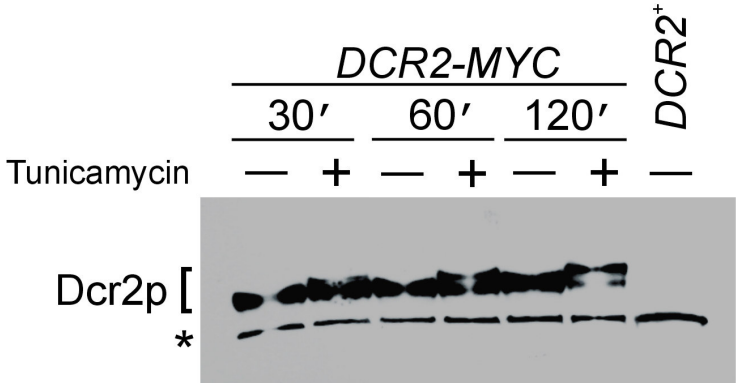

Figure 4.7 Dcr2p is modified under ER stress. The levels of Myc-tagged Dcr2p were evaluated by SDS-PAGE and immunoblotting, after exposure to tunicamycin for the indicated time. A non-specific band is designated with an asterisk (*), and indicates loading.

CHAPTER V

SUMMARY AND PROSPECTIVE STUDIES

The dissertation is composed of two parts:

PART ONE

All proliferating cells have to coordinate their overall growth with cell division. Tight coordination between cell growth and division determines when cells initiate cell division. Current models predict that only in the G1 phase of the cell cycle cells monitor their growth. In this study, we test these models using continuous chemostat cultures, where growth rate was varied independently of nutrient composition. First, during five different growth rates, cell size was constant in either glucose- or nitrogen-limitated continuous cultures, but it was different between the two nutrients. This indicates that cell size varies as a function of nutrient composition, but not as a function of growth rate. Second, during five different growth rates, the duration of the G1 phase only predominantly expands under glucose limitation as growth rate decreases, whereas all cell cycle phases proportionally expand under nitrogen limitation. This indicates that there are nutrient-specific effects on cell cycle progression, which are independent of growth rate. Together, these results strongly suggest that it is unlikely that in continuously proliferating cells “cell growth” is exclusively monitored at the START point of the cell cycle in G1.

PART TWO

The endoplasmic reticulum (ER) is not only a processing plant for the maturation of proteins but also the first compartment in the ordered membranous network for secretion, which is essential to all eukaryotic cells. The balance between the load of client proteins into the ER and the transportation of client proteins out of the ER is required for the normal physiological function of the ER. Perturbation to the ER homeostasis will result in the accumulation of unfolded proteins and cause ER stress. Eukaryotic cells, including budding yeast, turn on the unfolded protein response (UPR) signaling pathway to restore the homeostasis. Due to the anti-mitogenic effects of UPR signaling, cells have to turn it off ultimately. In this study, we demonstrate how the Dosage-dependent Cell cycle Regulator (Dcr2p) phosphatase down-regulates UPR signaling in *Saccharomyces cerevisiae*, using both genetic and biochemical approaches. First, a genome-wide genetic screen indicates that Dcr2p has a role in the unfolded protein response, because we identified interactions with nine known genes involved in secretion/UPR. We further confirmed the synthetic growth defects upon combined loss of *DCR2* and *IRE1*, the major initiator and transducer gene for UPR signaling. Second, over-expression of the catalytically active Dcr2p can antagonize UPR signaling under ER stress, by significantly attenuating *HAC1* mRNA splicing, the major transcription factor for activating UPR target genes. Lastly, Dcr2p physically interacts with Ire1p *in vivo* in an Ire1p phosphorylation dependent manner, and Dcr2p can directly de-phosphorylate autophosphorylated Ire1p *in vitro*. Together, these experiments support our model that Dcr2p targets Ire1p and downregulates the unfolded protein response in

Saccharomyces cerevisiae. Our results are significant because, for the first time, we have a mechanism of how to turn off the anti-mitogenic UPR signaling, by directly modulating Ire1p activity, the major component of the UPR.

In the future, it will be very interesting and meaningful to further pursue what kind of post-translational modifications of Dcr2p are under the ER stress, and how these modifications affect the function of Dcr2p on UPR signaling. The answers to these questions will likely help us understand what kind of feedback mechanism of ER stress to Dcr2p, which would present us more clues about how UPR modulation is achieved. In addition, further clarification of the roles of other potential phosphatase, such as Ptc1p, on UPR signaling will be very helpful for us to have a bigger picture of phosphatase on UPR signaling. The difference of how UPR signaling is downregulated (recovery of *HAC1* mRNA splicing and its translational block) between cells under the nutrient sensing and chemical induced ER stress implies that the modulation of UPR signaling is regulated in a subtle and signal-dependent manner, possibly through different mechanisms. The UPR signaling modulation is still mysterious. Because of the importance of modulating UPR signaling in pathology, works on this will have a great prospective significance.

REFERENCES

Aridor, M., and Balch, W. E. (1999). Integration of endoplasmic reticulum signaling in health and disease. Nat Med *5*, 745-751.

Arnold, E., and Tanner, W. (1982). An obligatory role of protein glycosylation in the life cycle of yeast cells. FEBS Lett *148*, 49-53.

Back, S. H., Schroder, M., Lee, K., Zhang, K., and Kaufman, R. J. (2005). ER stress signaling by regulated splicing: IRE1/HAC1/XBP1. Methods *35*, 395-416.

Bertolotti, A., Zhang, Y., Hendershot, L. M., Harding, H. P., and Ron, D. (2000). Dynamic interaction of BiP and ER stress transducers in the unfolded-protein response. Nat Cell Biol *2*, 326-332.

Bishop, A. C., Shah, K., Liu, Y., Witucki, L., Kung, C., and Shokat, K. M. (1998). Design of allele-specific inhibitors to probe protein kinase signaling. Curr Biol *8*, 257-266.

Bogomolnaya, L. M., Pathak, R., Cham, R., Guo, J., Surovtseva, Y. V., Jaeckel, L., and Polymenis, M. (2004a). A new enrichment approach identifies genes that alter cell cycle progression in *Saccharomyces cerevisiae*. Curr Genet *45*, 350-359.

Bogomolnaya, L. M., Pathak, R., Guo, J., Cham, R., Aramayo, R., and Polymenis, M. (2004b). Hym1p affects cell cycle progression in *Saccharomyces cerevisiae*. Curr Genet *46*, 183-192.

Bogomolnaya, L. M., Pathak, R., Guo, J., and Polymenis, M. (2006). Roles of the RAM signaling network in cell cycle progression in Saccharomyces cerevisiae. Curr Genet *49*, 384-392.

Brewer, J. W., and Diehl, J. A. (2000). PERK mediates cell-cycle exit during the mammalian unfolded protein response. Proc Natl Acad Sci USA *97*, 12625-12630.

Brewer, J. W., Hendershot, L. M., Sherr, C. J., and Diehl, J. A. (1999). Mammalian unfolded protein response inhibits cyclin D1 translation and cell-cycle progression. Proc Natl Acad Sci USA *96*, 8505-8510.

Bryan, B. A., McGrew, E., Lu, Y., and Polymenis, M. (2004). Evidence for control of nitrogen metabolism by a START-dependent mechanism in *Saccharomyces cerevisiae*. Mol Genet Genomics *271*, 72-81.

Calfon, M., Zeng, H., Urano, F., Till, J. H., Hubbard, S. R., Harding, H. P., Clark, S. G., and Ron, D. (2002). IRE1 couples endoplasmic reticulum load to secretory capacity by processing the XBP-1 mRNA. Nature *415*, 92-96.

Carter, B. L. A., and Jagadish, M. N. (1978). Control of cell division in the yeast *Saccharomyces cerevisiae* cultured at different growth rates. Exp Cell Res *112*, 373-383.

Chapman, R. E., and Walter, P. (1997). Translational attenuation mediated by an mRNA intron. Curr Biol *7*, 850-859.

Conlon, I., and Raff, M. (2003). Differences in the way a mammalian cell and yeast cells coordinate cell growth and cell-cycle progression. J Biol *2*, 7.

Cox, J. S., Shamu, C. E., and Walter, P. (1993). Transcriptional induction of genes encoding endoplasmic reticulum resident proteins requires a transmembrane protein kinase. Cell *73*, 1197-1206.

Cox, J. S., and Walter, P. (1996). A novel mechanism for regulating activity of a transcription factor that controls the unfolded protein response. Cell *87*, 391-404.

Credle, J. J., Finer-Moore, J. S., Papa, F. R., Stroud, R. M., and Walter, P. (2005). Inaugural Article: On the mechanism of sensing unfolded protein in the endoplasmic reticulum. Proc Natl Acad Sci USA *102*, 18773-18784.

Cross, F. R. (1988). *DAF1*, a mutant gene affecting size control, pheromone arrest, and cell cycle kinetics of *Saccharomyces cerevisiae*. Mol Cell Biol *8*, 4675-4684.

Dever, T. E. (2002). Gene-specific regulation by general translation factors. Cell *108*, 545-556.

Edwards, M. C., Liegeois, N., Horecka, J., DePinho, R. A., Sprague, G. F. J., Tyers, M., and Elledge, S. J. (1997). Human *CPR* (Cell Cycle Progression Restoration) genes impart a Far$^-$ phenotype on yeast cells. Genetics *147*, 1063-1076.

Geer, L. Y., Domrachev, M., Lipman, D. J., and Bryant, S. H. (2002). CDART: protein homology by domain architecture. Genome Res *12*, 1619-1623.

Gelperin, D. M., White, M. A., Wilkinson, M. L., Kon, Y., Kung, L. A., Wise, K. J., Lopez-Hoyo, N., Jiang, L., Piccirillo, S., Yu, H.*, et al.* (2005). Biochemical and genetic analysis of the yeast proteome with a movable ORF collection. Genes Dev *19*, 2816-2826.

Gething, M. J., and Sambrook, J. (1992). Protein folding in the cell. Nature *355*, 33-45.

Ghaemmaghami, S., Huh, W. K., Bower, K., Howson, R. W., Belle, A., Dephoure, N., O'Shea, E. K., and Weissman, J. S. (2003). Global analysis of protein expression in yeast. Nature *425*, 737-741.

Griffin, D., ed. (1994). Growth, In Fungal Physiology, (New York: Wiley-Liss), pp. 102-129.

Guo, J., Bryan, B. A., and Polymenis, M. (2004). Nutrient-specific effects in the coordination of cell growth with cell division in continuous cultures of *Saccharomyces cerevisiae*. Arch Microbiol *182*, 326-330.

Guo, J., and Polymenis, M. (2006). Dcr2 targets Ire1 and downregulates the unfolded protein response in Saccharomyces cerevisiae. EMBO Rep *7*, 1124-1127.

Guzman, L. M., Belin, D., Carson, M. J., and Beckwith, J. (1995). Tight regulation, modulation, and high-level expression by vectors containing the arabinose PBAD promoter. J Bacteriol *177*, 4121-4130.

Haase, S. B., and Lew, D. J. (1997). Flow cytometric analysis of DNA content in budding yeast. Methods Enzymol *283*, 322-332.

Han, B.-K., Aramayo, R., and Polymenis, M. (2003). The G1 cyclin Cln3p controls vacuolar biogenesis in *Saccharomyces cerevisiae*. Genetics *165*, 467-476.

Harding, H. P., Calfon, M., Urano, F., Novoa, I., and Ron, D. (2002). Transcriptional and translational control in the mammalian unfolded protein response. Annu Rev Cell Dev Biol *18*, 575-599.

Harding, H. P., Novoa, I., Bertolotti, A., Zeng, H., Zhang, Y., Urano, F., Jousse, C., and Ron, D. (2001). Translational regulation in the cellular response to biosynthetic load on the endoplasmic reticulum. Cold Spring Harb Symp Quant Biol *66*, 499-508.

Harding, H. P., Zhang, Y., and Ron, D. (1999). Protein translation and folding are coupled by an endoplasmic-reticulum-resident kinase. Nature *397*, 271-274.

Hartwell, L. H., and Unger, M. W. (1977). Unequal division in *Saccharomyces cerevisiae* and its implications for the control of cell division. J Cell Biol *75*, 422-435.

Haze, K., Yoshida, H., Yanagi, H., Yura, T., and Mori, K. (1999). Mammalian transcription factor ATF6 is synthesized as a transmembrane protein and activated by proteolysis in response to endoplasmic reticulum stress. Mol Biol Cell *10*, 3787-3799.

Hemminki, A., Markie, D., Tomlinson, I., Avizienyte, E., Roth, S., Loukola, A., Bignell, G., Warren, W., Aminoff, M., Hoglund, P.*, et al.* (1998). A serine/threonine kinase gene defective in Peutz-Jeghers syndrome. Nature *391*, 184-187.

Hendershot, L. M., Ting, J., and Lee, A. S. (1988). Identity of the immunoglobulin heavy-chain-binding protein with the 78,000-dalton glucose-regulated protein and the role of posttranslational modifications in its binding function. Mol Cell Biol *8*, 4250-4256.

Hori, O., Ichinoda, F., Yamaguchi, A., Tamatani, T., Taniguchi, M., Koyama, Y., Katayama, T., Tohyama, M., Stern, D. M., Ozawa, K.*, et al.* (2004). Role of Herp in the endoplasmic reticulum stress response. Genes Cells *9*, 457-469.

Iwakoshi, N. N., Lee, A. H., Vallabhajosyula, P., Otipoby, K. L., Rajewsky, K., and Glimcher, L. H. (2003). Plasma cell differentiation and the unfolded protein response intersect at the transcription factor XBP-1. Nat Immunol *4*, 321-329.

Jagadish, M. N., and Carter, B. L. A. (1977). Genetic control of cell division in yeast cultured at different growth rates. Nature *269*, 145-147.

Johnston, G. C., Ehrhardt, C. W., Lorincz, A., and Carter, B. L. A. (1979). Regulation of cell size in the yeast. Journal of Bacteriology *137*, 1-5.

Jorgensen, P., Nishikawa, J. L., Breitkreutz, B. J., and Tyers, M. (2002). Systematic identification of pathways that couple cell growth and division in yeast. Science *297*, 395-400.

Jorgensen, P., Rupes, I., Sharom, J. R., Schneper, L., Broach, J. R., and Tyers, M. (2004). A dynamic transcriptional network communicates growth potential to ribosome synthesis and critical cell size. Genes Dev *18*, 2491-2505.

Kaiser, C., Michaelis, S., and Mitchell, A. (1994). Methods in Yeast Genetics (Cold Spring Harbor, NY: Cold Spring Harbor Laboratory Press).

Kaufman, R. J. (1999). Stress signaling from the lumen of the endoplasmic reticulum: coordination of gene transcriptional and translational controls. Genes Dev *13*, 1211-1233.

Kaufman, R. J., Scheuner, D., Schroder, M., Shen, X., Lee, K., Liu, C. Y., and Arnold, S. M. (2002). The unfolded protein response in nutrient sensing and differentiation. Nat Rev Mol Cell Biol *3*, 411-421.

Kawahara, T., Yanagi, H., Yura, T., and Mori, K. (1997). Endoplasmic reticulum stress-induced mRNA splicing permits synthesis of transcription factor Hac1p/Ern4p that activates the unfolded protein response. Mol Biol. Cell *8*, 1845-1862.

Kozutsumi, Y., Normington, K., Press, E., Slaughter, C., Sambrook, J., and Gething, M. J. (1989). Identification of immunoglobulin heavy chain binding protein as glucose-regulated protein 78 on the basis of amino acid sequence, immunological cross-reactivity, and functional activity. J Cell Sci Suppl *11*, 115-137.

Kozutsumi, Y., Segal, M., Normington, K., Gething, M. J., and Sambrook, J. (1988). The presence of malfolded proteins in the endoplasmic reticulum signals the induction of glucose-regulated proteins. Nature *332*, 462-464.

Laemmli, U. K. (1970). Cleavage of structural proteins during the assembly of the head of bacteriophage T4. Nature *227*, 680-685.

Leber, J. H., Bernales, S., and Walter, P. (2004). IRE1-independent gain control of the unfolded protein response. PLoS Biol *2*, E235.

Lee, A. H., Iwakoshi, N. N., and Glimcher, L. H. (2003). XBP-1 regulates a subset of endoplasmic reticulum resident chaperone genes in the unfolded protein response. Mol Cell Biol *23*, 7448-7459.

Lee, A. S. (1992). Mammalian stress response: induction of the glucose-regulated protein family. Curr Opin Cell Biol *4*, 267-273.

Liu, C. Y., Schroder, M., and Kaufman, R. J. (2000). Ligand-independent dimerization activates the stress response kinases IRE1 and PERK in the lumen of the endoplasmic reticulum. J Biol Chem *275*, 24881-24885.

Lloyd, D., Lemar, K. M., Salgado, L. E., Gould, T. M., and Murray, D. B. (2003). Respiratory oscillations in yeast: mitochondrial reactive oxygen species, apoptosis and time; a hypothesis. FEMS Yeast Res *3*, 333-339.

Lloyd, D., and Murray, D. B. (2006). The temporal architecture of eukaryotic growth. FEBS Lett *580*, 2830-2835.

Ma, Y., Brewer, J. W., Diehl, J. A., and Hendershot, L. M. (2002). Two distinct stress signaling pathways converge upon the CHOP promoter during the mammalian unfolded protein response. J Mol Biol *318*, 1351-1365.

Mertz, P., Yu, L., Sikkink, R., and Rusnak, F. (1997). Kinetic and spectroscopic analyses of mutants of a conserved histidine in the metallophosphatases calcineurin and lambda protein phosphatase. J Biol Chem *272*, 21296-21302.

Mori, K., Ma, W., Gething, M. J., and Sambrook, J. (1993). A transmembrane protein with a cdc2+/CDC28-related kinase activity is required for signaling from the ER to the nucleus. Cell *74*, 743-756.

Mori, K., Ogawa, N., Kawahara, T., Yanagi, H., and Yura, T. (2000). mRNA splicing-mediated C-terminal replacement of transcription factor Hac1p is required for efficient activation of the unfolded protein response. Proc Natl Acad Sci U S A *97*, 4660-4665.

Mori, K., Sant, A., Kohno, K., Normington, K., Gething, M. J., and Sambrook, J. F. (1992). A 22 bp cis-acting element is necessary and sufficient for the induction of the yeast KAR2 (BiP) gene by unfolded proteins. Embo J *11*, 2583-2593.

Murray, A., and Hunt, T. (1993). The Cell Cycle (New York: Oxford University Press).

Nakagawa, T., Zhu, H., Morishima, N., Li, E., Xu, J., Yankner, B. A., and Yuan, J. (2000). Caspase-12 mediates endoplasmic-reticulum-specific apoptosis and cytotoxicity by amyloid-beta. Nature *403*, 98-103.

Nasmyth, K. A. (1979). A control acting over the initiation of DNA replication in the yeast *Schizosaccharomyces pombe*. J Cell Sci *36*, 155-168.

Neufeld, T. P., and Edgar, B. A. (1998). Connections between growth and the cell cycle. Curr Opin Cell Biol *10*, 784-790.

Nikawa, J., Akiyoshi, M., Hirata, S., and Fukuda, T. (1996). *Saccharomyces cerevisiae* IRE2/HAC1 is involved in IRE1-mediated KAR2 expression. Nucleic Acids Res *24*, 4222-4226.

Nishikawa, Y., Yamamoto, Y., Kaji, K., and Mitsui, H. (1980). Reversible G1 arrest of a human Burkitt lymphoma cell line(Raji) induced by tunicamycin. Biochem Biophys Res Commun *97*, 1296-1303.

Nishitoh, H., Matsuzawa, A., Tobiume, K., Saegusa, K., Takeda, K., Inoue, K., Hori, S., Kakizuka, A., and Ichijo, H. (2002). ASK1 is essential for endoplasmic reticulum stress-induced neuronal cell death triggered by expanded polyglutamine repeats. Genes Dev *16*, 1345-1355.

Niwa, M., Patil, C. K., DeRisi, J., and Walter, P. (2005). Genome-scale approaches for discovering novel nonconventional splicing substrates of the Ire1 nuclease. Genome Biol *6*, R3.

Nock, S., Gonzalez, T. N., Sidrauski, C., Niwa, M., and Walter, P. (2001). Purification and activity assays of the catalytic domains of the kinase/endoribonuclease Ire1p from *Saccharomyces cerevisiae*. Methods Enzymol *342*, 3-10.

Nojima, H., Leem, S. H., Araki, H., Sakai, A., Nakashima, N., Kanaoka, Y., and Ono, Y. (1994). Hac1: a novel yeast bZIP protein binding to the CRE motif is a multicopy suppressor for cdc10 mutant of *Schizosaccharomyces pombe*. Nucleic Acids Res *22*, 5279-5288.

Paalman, J. W., Verwaal, R., Slofstra, S. H., Verkleij, A. J., Boonstra, J., and Verrips, C. T. (2003). Trehalose and glycogen accumulation is related to the duration of the G1 phase of *Saccharomyces cerevisiae*. FEMS Yeast Res *3*, 261-268.

Papa, F. R., Zhang, C., Shokat, K., and Walter, P. (2003). Bypassing a kinase activity with an ATP-competitive drug. Science *302*, 1533-1537.

Pathak, R., Bogomolnaya, L. M., Guo, J., and Polymenis, M. (2004). Gid8p (Dcr1p) and Dcr2p function in a common pathway to promote START completion in *Saccharomyces cerevisiae*. Euk Cell *3*, 1627-1638.

Pathak, R., Bogomolnaya, L. M., Guo, J., and Polymenis, M. (2005). A role for KEM1 at the START of the cell cycle in *Saccharomyces cerevisiae*. Curr Genet *48*, 300-309.

Patil, C., and Walter, P. (2001). Intracellular signaling from the endoplasmic reticulum to the nucleus: the unfolded protein response in yeast and mammals. Curr Opin Cell Biol *13*, 349-355.

Patil, C. K., Li, H., and Walter, P. (2004). Gcn4p and novel upstream activating sequences regulate targets of the unfolded protein response. PLoS Biol *2*, E246.

Polymenis, M., and Schmidt, E. V. (1997). Coupling of cell division to cell growth by translational control of the G1 cyclin CLN3 in yeast. Genes Dev *11*, 2522-2531.

Polymenis, M., and Schmidt, E. V. (1999). Coordination of cell growth with cell division. Curr Opin Genet Dev *9*, 76-80.

Pouyssegur, J., Shiu, R. P., and Pastan, I. (1977). Induction of two transformation-sensitive membrane polypeptides in normal fibroblasts by a block in glycoprotein synthesis or glucose deprivation. Cell *11*, 941-947.

Prendergast, J. A., Murray, L. E., Rowley, A., Carruthers, D. R., Singer, R. A., and Johnston, G. C. (1990). Size selection identifies new genes that regulate *Saccharomyces cerevisiae* cell proliferation. Genetics *124*, 81-90.

Pringle, J. R., and Hartwell, L. H. (1981). The *Saccharomyces cerevisiae* cell cycle, In The Molecular Biology of the Yeast *Saccharomyces*, J. D. Strathern, E. W. Jones, and J. R. Broach, eds. (Cold Spring Harbor, NY: Cold Spring Harbor Laboratory Press), pp. 97-142.

Reed, S. I. (1980). The selection of *S. cerevisiae* mutants defective in the start event of cell division. Genetics *95*, 561-577.

Reimold, A. M., Iwakoshi, N. N., Manis, J., Vallabhajosyula, P., Szomolanyi-Tsuda, E., Gravallese, E. M., Friend, D., Grusby, M. J., Alt, F., and Glimcher, L. H. (2001). Plasma cell differentiation requires the transcription factor XBP-1. Nature *412*, 300-307.

Reimold, A. M., Ponath, P. D., Li, Y. S., Hardy, R. R., David, C. S., Strominger, J. L., and Glimcher, L. H. (1996). Transcription factor B cell lineage-specific activator protein regulates the gene for human X-box binding protein 1. J Exp Med *183*, 393-401.

Richmond, K. M., and Williamson, D. H. (1983). Residual cell division measurements are unreliable as indicators of the timing of events in the *Saccharomyces cerevisiae* cell cycle. J Cell Sci *64*, 307-322.

Ruegsegger, U., Leber, J. H., and Walter, P. (2001). Block of HAC1 mRNA translation by long-range base pairing is released by cytoplasmic splicing upon induction of the unfolded protein response. Cell *107*, 103-114.

Rutkowski, D. T., and Kaufman, R. J. (2004). A trip to the ER: coping with stress. Trends Cell Biol *14*, 20-28.

Savage, K. E., and Baur, P. S. (1983). Effect of tunicamycin, an inhibitor of protein glycosylation, on division of tumour cells *in vitro*. J Cell Sci *64*, 295-306.

Scheuner, D., Song, B., McEwen, E., Liu, C., Laybutt, R., Gillespie, P., Saunders, T., Bonner-Weir, S., and Kaufman, R. J. (2001). Translational control is required for the unfolded protein response and *in vivo* glucose homeostasis. Mol Cell *7*, 1165-1176.

Schneider, B. L., Zhang, J., Markwardt, J., Tokiwa, G., Volpe, T., Honey, S., and Futcher, B. (2004). Growth rate and cell size modulate the synthesis of, and requirement for, G1-phase cyclins at start. Mol Cell Biol *24*, 10802-10813.

Schroder, M., Chang, J. S., and Kaufman, R. J. (2000). The unfolded protein response represses nitrogen-starvation induced developmental differentiation in yeast. Genes Dev *14*, 2962-2975.

Schroder, M., Clark, R., and Kaufman, R. J. (2003). IRE1- and HAC1-independent transcriptional regulation in the unfolded protein response of yeast. Mol Microbiol *49*, 591-606.

Schroder, M., Clark, R., Liu, C. Y., and Kaufman, R. J. (2004). The unfolded protein response represses differentiation through the RPD3-SIN3 histone deacetylase. Embo J *23*, 2281-2292.

Shamu, C. E., and Walter, P. (1996). Oligomerization and phosphorylation of the Ire1p kinase during intracellular signaling from the endoplasmic reticulum to the nucleus. Embo J *15*, 3028-3039.

Shen, X., Ellis, R. E., Lee, K., Liu, C. Y., Yang, K., Solomon, A., Yoshida, H., Morimoto, R., Kurnit, D. M., Mori, K., and Kaufman, R. J. (2001). Complementary signaling pathways regulate the unfolded protein response and are required for C. elegans development. Cell *107*, 893-903.

Sidrauski, C., Cox, J. S., and Walter, P. (1996). tRNA ligase is required for regulated mRNA splicing in the unfolded protein response. Cell *87*, 405-413.

Sidrauski, C., and Walter, P. (1997). The transmembrane kinase Ire1p is a site-specific endonuclease that initiates mRNA splicing in the unfolded protein response. Cell *90*, 1031-1039.

Siniossoglou, S., Peak-Chew, S. Y., and Pelham, H. R. (2000). Ric1p and Rgp1p form a complex that catalyses nucleotide exchange on Ypt6p. Embo J *19*, 4885-4894.

Spode, I., Maiwald, D., Hollenberg, C. P., and Suckow, M. (2002). ATF/CREB sites present in sub-telomeric regions of *Saccharomyces cerevisiae* chromosomes are part of promoters and act as UAS/URS of highly conserved COS genes. J Mol Biol *319*, 407-420.

Strich, R., Surosky, R. T., Steber, C., Dubois, E., Messenguy, F., and Esposito, R. E. (1994). UME6 is a key regulator of nitrogen repression and meiotic development. Genes Dev *8*, 796-810.

Sudbery, P. E., Goodey, A. R., and Carter, B. L. (1980). Genes which control cell proliferation in the yeast *Saccharomyces cerevisiae*. Nature *288*, 401-404.

Tardif, K. D., Waris, G., and Siddiqui, A. (2005). Hepatitis C virus, ER stress, and oxidative stress. Trends Microbiol *13*, 159-163.

Tong, A. H., Evangelista, M., Parsons, A. B., Xu, H., Bader, G. D., Page, N., Robinson, M., Raghibizadeh, S., Hogue, C. W., Bussey, H., *et al.* (2001). Systematic genetic analysis with ordered arrays of yeast deletion mutants. Science *294*, 2364-2368.

Travers, K. J., Patil, C. K., Wodicka, L., Lockhart, D. J., Weissman, J. S., and Walter, P. (2000). Functional and genomic analyses reveal an essential coordination between the unfolded protein response and ER-associated degradation. Cell *101*, 249-258.

Tu, B. P., Kudlicki, A., Rowicka, M., and McKnight, S. L. (2005). Logic of the yeast metabolic cycle: temporal compartmentalization of cellular processes. Science *310*, 1152-1158.

Tu, B. P., and McKnight, S. L. (2006). Metabolic cycles as an underlying basis of biological oscillations. Nat Rev Mol Cell Biol *7*, 696-701.

Welihinda, A. A., and Kaufman, R. J. (1996). The unfolded protein response pathway in *Saccharomyces cerevisiae*. Oligomerization and trans-phosphorylation of Ire1p (Ern1p) are required for kinase activation. J Biol Chem *271*, 18181-18187.

Welihinda, A. A., Tirasophon, W., Green, S. R., and Kaufman, R. J. (1997). Gene induction in response to unfolded protein in the endoplasmic reticulum is mediated through Ire1p kinase interaction with a transcriptional coactivator complex containing Ada5p. Proc Natl Acad Sci USA *94*, 4289-4294.

Welihinda, A. A., Tirasophon, W., Green, S. R., and Kaufman, R. J. (1998). Protein serine/threonine phosphatase Ptc2p negatively regulates the unfolded-protein response by dephosphorylating Ire1p kinase. Mol Cell Biol *18*, 1967-1977.

Welihinda, A. A., Tirasophon, W., and Kaufman, R. J. (2000). The transcriptional co-activator ADA5 is required for HAC1 mRNA processing *in vivo*. J Biol Chem *275*, 3377-3381.

Wu, J., and Kaufman, R. J. (2006). From acute ER stress to physiological roles of the unfolded protein response. Cell Death Differ *13*, 374-384.

Yoshida, H., Haze, K., Yanagi, H., Yura, T., and Mori, K. (1998). Identification of the cis-acting endoplasmic reticulum stress response element responsible for transcriptional induction of mammalian glucose-regulated proteins. Involvement of basic leucine zipper transcription factors. J Biol Chem *273*, 33741-33749.

Yoshida, H., Okada, T., Haze, K., Yanagi, H., Yura, T., Negishi, M., and Mori, K. (2000). ATF6 activated by proteolysis binds in the presence of NF-Y (CBF) directly to the cis-acting element responsible for the mammalian unfolded protein response. Mol Cell Biol *20*, 6755-6767.

Zettel, M. F., Garza, L. R., Cass, A. M., Myhre, R. A., Haizlip, L. A., Osadebe, S. N., Sudimack, D. W., Pathak, R., Stone, T. L., and Polymenis, M. (2003). The budding index of *Saccharomyces cerevisiae* deletion strains identifies genes important for cell cycle progression. FEMS Microbiol Lett *223*, 253-258.

Zhang, J., Schneider, C., Ottmers, L., Rodriguez, R., Day, A., Markwardt, J., and Schneider, B. L. (2002). Genomic scale mutant hunt identifies cell size homeostasis genes in *S. cerevisiae*. Curr Biol *12*, 1992-2001.

Zhang, K., and Kaufman, R. J. (2004). Signaling the unfolded protein response from the endoplasmic reticulum. J Biol Chem *279*, 25935-25938.

Zhou, J., Liu, C. Y., Back, S. H., Clark, R. L., Peisach, D., Xu, Z., and Kaufman, R. J. (2006). The crystal structure of human IRE1 luminal domain reveals a conserved dimerization interface required for activation of the unfolded protein response. Proc Natl Acad Sci USA *103*, 14343-14348.

Zhuo, S., Clemens, J. C., Stone, R. L., and Dixon, J. E. (1994). Mutational analysis of a Ser/Thr phosphatase. Identification of residues important in phosphoesterase substrate binding and catalysis. J Biol Chem *269*, 26234-26238.

VITA

Name: Jinbai Guo

Address: Department of Biochemistry
TAMU MS 2128
College Station, TX 77843

Email Address:gjbwj@tamu.edu

Telephone: 979-458-3261 (lab)

Education: B.S., Biotechnology, 1993, Northeast Agriculture University, Harbin, China.
M.S., 2001, Pharmacology, Harbin Medical University, Harbin, China
Ph.D., 2007, Genetics, Texas A&M University, Texas, USA